

**OPTIMIZATION OF ELECTRON BEAM LITHOGRAPHY AND LIFT-OFF  
PROCESS FOR NANOFABRICATION OF SUB-50 NM GOLD  
NANOSTRUCTURES**

by  
OSMAN ŞAHİN

Submitted to the Graduate School of Engineering and Natural Sciences  
in partial fulfilment of  
the requirements for the degree of Master of Science

Sabancı University  
December 2019

**OPTIMIZATION OF ELECTRON BEAM LITHOGRAPHY AND LIFT-OFF  
PROCESS FOR NANOFABRICATION OF SUB-50 NM GOLD  
NANOSTRUCTURES**

Approved by:

Asst. Prof. Dr. Murat Kaya Yapıcı  
(Thesis Supervisor)



Assoc. Prof. Dr. Meltem Sezen



Prof. Dr. Arda Deniz Yalçınkaya



Approval Date: December 9, 2019

OSMAN ŞAHİN 2019 ©

All Rights Reserved

## ABSTRACT

### OPTIMIZATION OF ELECTRON BEAM LITHOGRAPHY AND LIFT-OFF PROCESS FOR NANOFABRICATION OF SUB-50 NM GOLD NANOSTRUCTURES

OSMAN ŞAHİN

ELECTRONICS ENGINEERING M.Sc. THESIS, DECEMBER 2019

Thesis Supervisor: Asst. Prof. Dr. Murat Kaya Yapici

Keywords: Electron-Beam Lithography, PMMA, Lift-Off, Gold Nanostructure,  
Nanofabrication, SEM

Since the demonstration of the first integrated circuit in the late 1950s, the microelectronics industry has witnessed a vast transformation with transistor densities doubling roughly every two years as a result of continuous scaling down of device dimensions, referred to as miniaturization. The fundamental concept of miniaturization has not only been employed for the realization of ultra large scale integrated (ULSI) circuits with reduced manufacturing costs, lower power consumption, higher speed and computational power; but also, for developing novel transducer elements and energy storage devices by harnessing the unique physical effects that arise at micro/nanoscales such as higher surface-to-volume ratios. One of the most important technologies in micro/nano device fabrication, if not the single most important, is lithography. The broad range of lithographic techniques ranging from conventional optical lithography methods (e.g. ultraviolet-UV, deep ultraviolet-DUV, extreme ultraviolet-EUV) to unconventional ones (e.g. electron beam lithography, x-ray lithography, ion-beam lithography, stereolithography, scanning probe lithography, nanoimprint lithography, directed self-assembly) can be used to create features with microns to tens of nanometer resolution and below. Among these, electron beam lithography (EBL) stands out as a powerful direct-write tool offering nanometer scale patterning capability and is especially useful in low volume R&D prototyping. However, patterning with EBL requires careful balance of process parameters which need to be considered in conjunction with the pattern transfer

technology that can be either etching or lift-off specifically for the case metallic layers. Accordingly, this thesis provides a systematic study to address the gap in process optimization of lift-off process based on EBL patterning of sub-50 nm metallic nanostructures using a lower cost PMMA/PMMA positive tone bilayer resist spin approach. The governing parameters in EBL including exposure dose, bake temperature, develop time, developer solution, substrate effect, proximity effect (PE) are experimentally studied and their effects on nanopatterning are characterized by field emission scanning electron microscopy (FE-SEM) of fabricated nanostructures.

## ÖZET

### 50 NM ALTINDA ALTIN NANOYAPILARIN NANOFABRİKASYONU İÇİN ELEKTRON DEMETİ LİTOGRAFI VE YÜZEYDEN KALDIRMA SÜREÇLERİNİN OPTİMİZASYONU

OSMAN ŞAHİN

ELEKTRONİK MÜHENDİSLİĞİ YÜKSEK LİSANS TEZİ, ARALIK 2019

Tez Danışmanı: Dr. Öğr. Üyesi Murat Kaya Yapıcı

Anahtar Kelimeler: Elektron Demeti Litografi, PMMA, Yüzeyden Kaldırma, Altın  
Nanoyapı, Nanoüretim, SEM

1950'lerin sonunda ilk entegre devrenin gösterilmesinden bu yana, minyatürleştirme olarak adlandırılan; cihaz boyunun sürekli azalması sonucu, mikro elektronik endüstrisi, transistor yoğunluğunun her iki yılda iki katına çıkmasına tanık olmaktadır. Minyatürleştirmenin temel konsepti yalnızca düşük üretim maliyeti, düşük güç tüketimi, daha yüksek hız ve hesaplama gücü ile ultra büyük ölçekli entegre (ULSI) devrelerin gerçekleştirilmesi için kullanılmadı; aynı zamanda, daha yüksek yüzey/hacim oranları gibi mikro/nano ölçeklerde ortaya çıkan benzersiz fiziksel etkileri de kullanarak yeni dönüştürücü elemanları ve enerji depolama cihazları geliştirmektir. Mikro/nano cihaz üretiminde en önemli teknolojilerden biri; en önemlisi olmasa da litografidir. Geleneksel optik litografi yöntemlerinden (örneğin; Ultraviyole-UV, derin ultraviyole (DUV), yoğun ultraviyole (EUV)) geleneksel olmayan yöntemlere (örneğin. Elektron demeti litografisi, x-ışını litografisi, iyon-ışın litografisi, stereolitografisi, tarama probu litografisi, nanobaskı litografisi, kendi kendine birleşme) kadar geniş çeşitli litografik teknikleri, onlarca mikron ve nanometre altındaki çözünürlüğü oluşturmak için kullanılabilir. Bunlar arasında, elektron demeti litografisi (EBL), nanometre ölçeği yazdırma yeteneği sunan güçlü direk yazma aracı olarak öne çıkmakta ve özellikle düşük hacimli Ar-Ge prototipleşmesinde yararlıdır. Ama, EBL yöntemi ile yazdırma süreç parametrelerinin, özellikle metalik katmanlar durumu için aşındırma veya yüzeyden kaldırma desen transfer teknolojisi ile birlikte düşünülmesi gereklidir. Bu yüzden, bu tez, daha düşük maliyetli bir PMMA/PMMA pozitif tonlu iki tabakalı resist'in kullanarak, 50 nm boyut altındaki

metalik nanoyapıların EBL yazdırmaya dayalı yüzeyden kaldırma sürecindeki optimizasyonundaki boşluğu ele almak için sistematik bir çalışma sunmaktadır. Pozlama dozu, pişirme sıcaklığı, yıkama süresi, yıkama çözeltisi, altaş etkisi, yakınlık etkisi (PE) dahil olmak üzere, EBL parametreleri deneysel olarak incelenecek ve nano yazdırma üzerindeki etkileri, alan emisyonu taramalı elektron mikroskopisi (FE-SEM) ile karakterize edilecektir.

## ACKNOWLEDGEMENTS

I would like to thank Asst. Prof. Dr. Murat Kaya Yapıcı who has been my advisor for all these years. When I started the fabrication process, I was an inexperienced and unskilled student. However, with his encouragement, supports and guidance, I have improved myself progressively. He has opened my ways to explore many areas freely. I have tried not to disappoint him. I hope I have met his expectations for all these years. It is an honour for me to meet him.

I would like to thank Assoc. Prof. Dr Meltem Sezen and Prof. Dr. Arda Deniz Yalçinkaya for being members of my thesis committee. I am also grateful to meet Prof. Dr. Mehmet Ali Gülgün for teaching me how to use Field-Emission Scanning Electronics Microscopy (FE-SEM) and sharing his valuable opinion with me. Thanks are to Asst. Prof. Dr. Meltem Elitaş for helping and directing me to find a correct source, especially when I took her course.

I have special thanks to Dr. Gülcan Çorapçioğlu for generous supports FE-SEM training, Nurel Karakaya for sharing her knowledge about usage of Fourier-transform infrared spectroscopy (FTIR), Onur Serbest to kindly teach me how to use cleanroom facilities and Bülent Köroğlu, Serkan Boston, Süleyman Çelik and Hasan Özkaya for their valuable and educational supports and assistances in the cleanroom. I thank Dr. Cenk Yanık who taught me how to use e-beam lithography provided me with a lot of freedom as using EBL and behaved toward me very friendly. Without their bits of help, supports, and guidance, it is not possible to fabricate and continue the process in the cleanroom easily.

I owe special thanks to my family. My beloved mother, Gülay, you are the person who is one of the leading roles in my life. You have provided me with courage, happiness, and supports until now. My beloved family members who are grandfather, grandmother, aunt, nephews, sister, and my little sweet nephew, Yağmur, no words could express my thanks and love towards you. I want to also thank you, my dear father, rest in peace!

I feel very lucky having a funny, knowledgeable, supportive and helpful teammate. It is hard to express your friendship and attitude towards me with words. I want to express special thanks to Gizem Acar for her constant support and friendship. We have spent enjoyable and instructive time, shared many happiness and sadness conditions since I met her at the first moment which was very funny ☺. I have thanks to my roommate and lab mate Melih Can Taşdelen to create my freedom in the room and to advise and support me. I would like also to thank Rayan Bajwa and Farid Sayar Irani for making me guidance in the cleanroom and relaxing me in case of my unhappiness moments. Thanks are to my other colleagues Ata Jedari Golparvar, Abdul Rahman Dabbour and Özberk Öztürk for gentle and valuable behaviour toward me, sharing their useful information with me. Although Tuğçe Delipinar and Heba Ahmed Sales are newcomers for our team, I built a good relationship with them due to their kindly and friendly behaviour as if they are joined our group two years ago. Mehve, you are very cute and colourful cat.

I want to express thanks for Ali Kasap and Sercan Tanyeli for supporting me during the master study. As the last word, a human being has learned many things by making many mistakes. If I break your hearts unintentionally during the learning process, I want to apologize to everyone to obey my life motto “don't make someone else anything you don't want to be done to you ”

*To my lovely family and women exposed to different types of violence and killed by  
brutal men*

.  
. .  
*Beni güzel hatırla*  
*Sayfalarca mektup bıraktım sana*  
*Şiirler yazdım her gece*  
*Çoğunu okutmadım*  
*Sakladım günahını sevabını içimde*  
*Sessizce gittim senden öncekiler gibi sende anlamadın*

.  
. .  
*Orhan Veli Kanık*

## TABLE OF CONTENTS

CHAPTER I.....	1
INTRODUCTION AND MOTIVATION .....	1
1.1. Introduction.....	1
1.2. Summary of Works .....	3
CHAPTER II.....	5
BACKGROUND ON NANO FABRICATION AND NANOTECHNOLOGY .....	5
2.1. Nanotechnology and Nanofabrication .....	5
2.2. Lithography .....	7
2.2.1. Lithographic Process.....	8
2.2.2. Types of Lithography.....	9
CHAPTER III .....	13
ELECTRON BEAM LITHOGRAPHY AND IRRADIATION OF RESIST .....	13
3.1. Electron Beam Lithography .....	13
3.2. Electron Beam Resist.....	16
3.2.1. Charge Dissipation.....	18
3.2.2. Positive Resist.....	18
3.2.3. Negative Resist .....	21
3.3. Parts of E-Beam Lithography Machine .....	22
3.3.1. E-Beam Lithography Column.....	23
3.3.2. Mechanical System .....	27
3.3.3. Vacuum System .....	27

3.3.4	Computer .....	28
3.4	Terminology.....	28
3.4.1	Writing Field.....	28
3.4.2	Stitching .....	28
3.4.3	Exposure Element .....	28
3.4.4	Exposure Dosage .....	29
3.4.5	System Clock .....	29
3.4.6	Proximity Effect.....	29
3.4.7	Beam Current.....	29
3.5	Conceptual Flow .....	30
3.5.1	Conceptual Design .....	30
3.5.2	CAD Design.....	30
3.5.3	Conversion and Proximity Effect .....	31
3.5.4	Sample Preparation .....	31
3.5.5	Exposure .....	32
3.5.6	Development .....	32
3.6	Electron-Solid Interaction .....	32
3.6.1	Forward Scattering.....	33
3.6.2	Backscattering.....	33
3.6.3	Secondary Electrons .....	33
3.7	Proximity Effect.....	34
3.7.1	Ways to Protection of Proximity Effect.....	35
3.8	Multilayer Systems .....	36
3.8.1	Low/High Molecular Weight PMMA.....	36
3.8.2	PMMA/Copolymer .....	36
3.8.3	Trilayer System.....	37
CHAPTER IV	.....	38

RELATED WORKS .....	38
CHAPTER V .....	46
NANOFABRICATION RESULTS .....	46
5.1. Nanofabrication.....	46
5.2 Wafer Preparation and Cleaning .....	46
5.3 Electron Beam Lithography .....	47
5.4 Discussion of Parameters .....	51
5.4.1 Exposure Dose .....	51
5.4.2 Development Time .....	55
5.4.3 Developer Concentration .....	58
5.4.4 Bake Temperature .....	60
5.4.5 Substrate Effect.....	61
5.4.6 PEC Effect .....	63
CHAPTER VI.....	66
CONCLUSIONS .....	66
BIBLIOGRAPHY .....	69
APPENDIX A .....	75
OPERATING PROCEDURE FOR VISTEC EBPG 5000+ES .....	75

## LIST OF TABLES

Table 3.1 Theoretical spot size for 100 kV <sup>1</sup> .....	16
Table 3.2 Comparison of commercially available electron beam resists [24,36].....	22
Table 3.3 Type of electron guns [24].....	24
Table 5.1 Specific parameters for Vistec EBPG500+ EBL .....	48
Table 5.2 List of commonly used composition and their effect on resolution and sensitivity [41] .....	59

## LIST OF FIGURES

Figure 2.1 Patterning techniques; a) Contact Printing, b) Proximity Printing, c) Projection Printing [30] .....	11
Figure 3.1 Schematic for positive and negative resists [9] .....	14
Figure 3.2 Relation of the beam and pixel size; a) Beamwidth too small for pixel width, pattern not fully exposed, b) Beamwidth too large for pixel width, pattern washed out, c) Good pixel/beam size ratio, the pattern is evenly exposed .....	15
Figure 3.3 Edge profile in positive resist [39] .....	19
Figure 3.4 PMMA reaction mechanism [24] .....	20
Figure 3.5 Negative profile after exposure [39] .....	21
Figure 3.6 Block diagram representing basic components of typical electron beam lithography [11] .....	23
Figure 3.7 Electron gun with a thermal field emission gun [11]. .....	24
Figure 3.8 Scanning methodologies for the beam of the electron: a) raster scan and b) vector scan [11].....	26
Figure 3.9 Schematic drawing of electrostatic deflectors [11] .....	26
Figure 3.10 Schematic drawing of beam axis-alignment coils [11]. .....	27
Figure 3.11 Diagram for some of the basic things for EBL .....	30
Figure 3.12 Schematic drawing for demonstrating the electron scattering for 30 keV and 100 keV on a silicon substrate [11]. .....	34
Figure 3.13 Simulation of proximity correction algorithm.....	35
Figure 3.14 Two bilayer e-beam resist structure a) High MW PMMA / Low MW PMMA b) PMMA /Copolymer c) The resist is then removed in the solvent. d) Final structure after dissolving resist [32]......	37
Figure 4.1 a) SEM images of the gaps using different electron doses 210, 220, and 230 mC/cm <sup>2</sup> , but same developing time of 60 s b) SEM of the gaps using different developing time doses 80, 120 and 180 s, but same electron doses 230 mC/cm <sup>2</sup> from top to bottom [46] .....	39

Figure 4.2 a) Nanohole array and c) Undercut profile for Nanoslit array after metal deposition b) and d) After lift-off for nanoholes and nanoslits. (e) and (f) Before and after lift-off cross-section view of the nanoslits configuration. Wide of the split is 100 nm wide, 100 nm thick; the pitch of split is 400 nm apart [47].....	40
Figure 4.3 Features of exposed patterns: (a) width and (b) depth for low- and high-voltage EBL for 1 and 10 kV and resist thicknesses for 30 nm and 300 nm, c) depth and d) width for acceleration voltages of up to 5 kV and resist thickness of 600 nm, e) various aperture sizes for 2 kV and 5kV, f) various baking temperatures [49].....	41
Figure 4.4 SEM image of a) sub-10 nm lines obtained by lift-off of a gold film, b) 20-nm line and space array [51].....	42
Figure 4.5 SEM images of lines and spaces with the dimension of a) 250 nm with a dose of 160 $\mu\text{C}/\text{cm}^2$ and thickness of resist 800 nm, b) 150 nm with a dose of 200 $\mu\text{C}/\text{cm}^2$ and thickness of resist 800 nm, c) 80 nm with a dose of 120 $\mu\text{C}/\text{cm}^2$ and thickness of resist 180 nm [52] .....	43
Figure 4.6 SEM image of 80 nm pitch in PMMA with 4 nm linewidth [54] .....	44
Figure 4.7 SEM image of nanobowtie structures using bilayer resist [12].....	45
Figure 5.1 Summary of nanofabrication process flow .....	49
Figure 5.2 Optical images of the dose spectrum.....	50
Figure 5.3 Schematic explanation of fabrication mechanism.....	52
Figure 5.4 SEM images of the gap nanostructures fabricated with the same development time for predesigned 40 and 50 nm gaps with various exposed dose values respectively; a) and b) 550 $\mu\text{C cm}^{-2}$ , c) and d) 700 $\mu\text{C cm}^{-2}$ , e) and f) 800 $\mu\text{C cm}^{-2}$ for substrate of silicon with a 500 nm thick layer of PECVD nitride.....	53
Figure 5.5 SEM images of the gap nanostructures fabricated the same developing time and type for predesigned 40 nm and 50 gaps with various exposed dose values respectively; a) and b) 550 $\mu\text{C cm}^{-2}$ , c) and d) 700 $\mu\text{C cm}^{-2}$ , e) and f) 800 $\mu\text{C cm}^{-2}$ for substrate of silicon .....	54
Figure 5.6 SEM images of the fabricated wires nanostructures with the same development time and type, but different doses of a) 550 $\mu\text{C cm}^{-2}$ b) 700 $\mu\text{C cm}^{-2}$ c) 800 $\mu\text{C cm}^{-2}$ for substrate of glass .....	55
Figure 5.7 SEM images of the fabricated predesign 40 nm and 50 nm gap nanostructures with the same exposure dose 550 $\mu\text{C cm}^{-2}$ and development type (MIBK: IPA (1:3)), but different development time respectively; a) and b) 210s, c) and d) 300 s, e) etched	

sidewall of wire exposed with $800 \mu\text{C cm}^{-2}$ in glass substrate with 300 s. ....	57
Figure 5.8 SEM images of the fabricated gap nanostructures with the same exposure dose, $800 \mu\text{C cm}^{-2}$ and, MIBK: IPA (1:3) and (1:1), but different development time respectively; a) 60 s and 5 s, b) 100 s and 5 s in the substrate of silicon.....	58
Figure 5.9 SEM images of the fabricated predesign 40 and 50 nm gap nanostructures with the same exposure dose, $800 \mu\text{C cm}^{-2}$ and same development time sequentially, but different development types of a) and b) only (MIBK: IPA (1:3) ), c) and d) (MIBK: IPA (1:3) and MIBK: IPA (1:1)) in the substrate of silicon with a 500 nm thick layer of PECVD nitride.....	60
Figure 5.10 SEM images of the fabricated gap nanostructures with the same exposure dose ( $550 \mu\text{C cm}^{-2}$ ), development type (MIBK: IPA (1:3)) and development time, but different bake temperature, respectively; a) $160^\circ\text{C}$ b) $180^\circ\text{C}$ in the substrate of glass .	61
Figure 5.11 SEM images of substrate type on linewidth when the exposure dose ( $700 \mu\text{C cm}^{-2}$ ), developer type (MIBK:IPA (1:3)) and (MIBK:IPA (1:1)) and develop time are kept constant for a) silicon and b) glass substrate. ....	62
Figure 5.12 SEM images of substrate type on linewidth when the exposure dose ( $550 \mu\text{C cm}^{-2}$ ), develop type (MIBK:IPA (1:3) and MIBK: IPA (1:1)) and time is kept constant for a) silicon and b) $\text{Si}_3\text{N}_4$ on bare silicon.....	63
Figure 5.13 SEM images of PEC on gap nanostructures when the exposure dose ( $550 \mu\text{C cm}^{-2}$ ), developer type (MIBK:IPA (1:3)) and (MIBK:IPA (1:1)) and develop time are kept constant for a) and b) no PEC , c) and d) PEC for silicon substrate.....	64
Figure 5.14 SEM images of the fabricated predesign wire nanostructures with the same development type (MIBK: IPA (1:3)), no PEC, exposure dose $800 \mu\text{C cm}^{-2}$ but different development time, respectively; a) 130 s, b) 180 s, c) 210 s, substrate of silicon with a 500 nm thick layer of PECVD nitride.....	65
Figure 5.15 SEM images of the fabricated predesign 40 and 50 nm gap nanostructures with the same development type (MIBK: IPA (1:3)), PEC, exposure dose $800 \mu\text{C cm}^{-2}$ , development time 180s in the substrate of silicon with a 500 nm thick layer of PECVD nitride.....	65

## LIST OF ABBREVIATIONS

EBL: Electron Beam Lithography.....	2
NIL: Nanoimprinting Lithography .....	2
PMMA: Poly(methyl methacrylate).....	2
HSQ: Hydrogen Silsesquioxane.....	2
PE: Proximity Effect.....	3
FE-SEM: Field Emission Scanning Electron Microscopy.....	3
PEC: Proximity Effect Correctio.....	4
NEMS: Nanoelectromechanical Systems.....	6
AFM: Atomic Force Microscopy.....	6
STM: Scanning Tunnelling Microscope.....	6
RIE: Reactive Ion Etching .....	7
FIB: Focus Ion Beam Lithography .....	8
UV: Ultra Violet .....	9
NA: Numerical Aperture .....	10
DF: Depth of Field.....	11
PDMS: Poly (dimethylsiloxanes) .....	12
MIBK: Methyl Isobutyl Ketone.....	13
HMW: High Molecular Weight.....	22
LMW: Low Molecular Weight.....	22
IPA: Isopropyl Alcohol .....	22
TMAH: Tetramethylammonium Hydroxide.....	22
DAC: Digital to Analog Converter.....	28
EXELs: Exposure Elements .....	28
FS: Forward Scattering.....	33
BS: Back Scattering.....	33
SE: Secondary Electron.....	33
ICP-RIE: Inductively coupled plasma reactive ion etching.....	39

SOI: Silicon on Insulator .....	40
CD: Critical Dimension.....	51
PECVD: Plasma-Enhanced Chemical Vapor Deposition.....	52
BSE: Backscattering Electron .....	62
FSE: Forward Scattering Electron .....	62
PSF: Point of Spread Function.....	68

## LIST OF EQUATIONS

Equation.1 Resolution Equation .....	10
Equation.2 Minimum Feature Size Equation.....	10
Equation.3 Numerical Aperture Equation .....	10
Equation.4 Depth of Focus Equation .....	11
Equation.5 Area Dose Equation .....	15
Equation.6 Line Dose Equation.....	15
Equation.7 Dot Equation .....	15
Equation.8 Contrast Equation .....	17
Equation.9 Forward Scattering Equation .....	33

## CHAPTER I

### INTRODUCTION AND MOTIVATION

#### 1.1. Introduction

According to the observation of Gordon Moore in 1965, the number of transistors in each sensor can be doubled for nearly every two years [1]. In light of Moore's law, microelectronics industries have directed themselves at scaling down device sizes to the nanoscale with a strong desire to succeed higher device performance [1]. That novelty in terms of reducing the dimension of the device has also offered an invitation to explore the broad spectrum in different fields like physics, quantum electronics, biology. After making some industrial and academic researches which show us the benefits of scaling down device sizes such as saving the amount of material, energy and time consumption, performance improvements [2], miniaturization has been popular among electronics industries. To fabricate such a small feature size, innovation in nanotechnology has been performed in terms of research and technology development at the atomic and molecular levels [3]. The main desire of nanotechnology is to fabricate and use nanostructures in interdisciplinary fields and then to provide control over matter, devices, and structures. Based on the improvements of nanoscale level, various fields such as electronics [4], material size, chemicals [5] [6], biology [7], which have been endeavoured to reach the nano-level, have much more request to explore the world of nanoscience. Since nanoscale devices can offer some unique properties such as thermoelectric properties, quantum size effects, the surface to volume ratio, easily integrated to the available system, cost reduction [8], miniaturization has been an attractive area for many years.

Many works for nanodevices have been related to finding new fabrication methods. Their fabrications are categorized into two stages. ‘Top-down approach’, first one, deals with different methods (e.g. Electron Beam Lithography (EBL), Photolithography and Nanoimprinting Lithography (NIL)) which are based on reduction of dimensions progressively [9]. ‘Bottom-up approach’, second technique, is another related technique (e.g. molecular self-assembly, carbon nanotube synthesis) which nanostructures are combined with smaller units such as atoms or molecules [9].

Lithography is the process in which patterns are imprinted from one medium to another. The ability of a conventional ultraviolet lithography system is not capable to fabricate nanoscale structures due to its diffraction limitation related to the wavelength of light [10]. Although enhancements for optical lithography have been implemented by decreasing wavelength to make possible for small structures, optical lithography usually starts to encounter difficulties related to shallow focus length and materials (e.g. resist, mask vs.) [11].

Among non-optical lithography techniques, EBL is one of the candidates to generate nanostructures with dimensions well below the optics resolution limit and it seems as if it has remained as a powerful tool in nanofabrication. EBL has a short wavelength of electrons and the capability of efficient focusing [12] and can be performed to fabricate nanostructures sub-50 nm by transferring electron energy to sensitive polymer based on the designed software mask. EBL resists are classified into two groups; one contains PMMA [13], PMMA/MAA [13], HSQ [14] and ZEP [13], etc. The other one called chemically amplified resists, includes UV111 [15], UV116 [15], SU-8 [5][16]. The primary resist in this thesis is polymethyl-methacrylate (PMMA), which is a positive photoresist and exists in the different forms in terms of solvent, concentration, and molecular weight. In EBL, however, the changes in the critical dimension of the patterns are restricted by some parameters such as electron scattering in the resist, type of substrate, development time, exposure dose vs. These issues placed limitations for small structures and so, must be considered when using the EBL system at 100 keV.

Main motivation of this thesis is to provide a systematic study to demonstrate the effects of several parameters (e.g. exposure dose, baking temperature, development time, developer solution, substrate effect, proximity effect (PE)) involved EBL performance and to determine an optimized process that can yield successful and repeatable patterning of sub-50 nm gold nanostructures based on lift-off strategy. Since during the layout process, geometrical parameters of nanostructures are fixed, as optimizing the fabrication conditions, being fabricated structures with minimum standard deviation and achieving repeatable results in terms of device dimension are possible to a great extent. Using low-cost polymethyl methacrylate (PMMA) resist categorized under molecular weights, concentration rate, and casting solvent, makes an easy lift-off process, which is the removal of both resist and metallic layer together by achieving undercut resist profile. After all fabrication processes, characterization for nanostructures will be performed by field emission scanning electron microscopy (FE-SEM) imaging desired nanometer size.

## **1.2. Summary of Works**

In this thesis, we present how to fabricate gold sub-50 nm structures by EBL and lift-off cheaply and then to make some optimizations for parameters of fabrication to see their effect on the fabrication process. A summary for each of the following chapters is given as follows:

Chapter 2 introduces some background of nanotechnology and mentions different types of techniques for nanofabrication. We present definitions, features, and types of lithography.

Chapter 3 describes the physical and theoretical features of EBL, which are used during the thesis, are discussed. Different types of e-beam resist are classified based on their chemical features, and various resist profiles are explained. Lastly, electron-solid interaction and different types of scattering are discussed in detail and some methods are suggested to minimize scattering effect on the resist. Chapter 4 demonstrates works existed in the literature and summarizes them

Chapter 5 describes the basic fabrication process and discusses their results together with its parameters. Then, we present some parameters (exposure dose, developer type, and development type, substrate effect, and bake temperature, proximity effect(PE)) to see their effects on obtaining final structures. These comparisons are supported by field emission scanning electron microscopy (FE-SEM). Chapter 6 discusses obtaining the results

## CHAPTER II

### **BACKGROUND ON NANO FABRICATION AND NANOTECHNOLOGY**

#### **2.1. Nanotechnology and Nanofabrication**

Control and manipulation of matter at the nanoscale is the main ability for nanotechnology which covers design, production, characterization, and application from submicron to atomic dimension [17]. Nanotechnology is evolved from microtechnology by shrinking device dimension to obtain faster, more powerful and less power consumption devices more than microelectronics [4]. Nanoscience and nanotechnology are working together to build up such a tiny thing. Management of materials at atomic, molecular and macromolecular scales whose properties are different than larger scale is the work in the field of nanoscience [18]. It can attain properties (e.g. optical, electrical and mechanical) from the bulk. On the other hand, nanotechnology can direct these materials at designing and fabricating the structures and then characterizing the results. Nanotechnology is the practical use of nanoscience at industrial and commercial objectives [18]. It is seen that nanotechnology and nanoscience feed to each other indissolubly.

There are many reasons why nanoscience and nanotechnology are so special. Firstly, at the nanoscale, the properties of the material are changed. This is the result of the small size of nanomaterials, explained as quantum effect physically which means that by decreasing the size of materials to the nanoscale, it leads to discrete energy levels depending on the size of the structure because of the confinement of movement of the electrons [19]. When the material reaches the nanoscale level, electrical conductivity, colour, strength change, which intend that same material, can be evaluated as

semiconductor or insulator at the nanoscale level. For example; bulk silver is considered as non-toxic, but silver particles can kill viruses once contacted [18]. The second reason is that atoms and molecules are utilized to build up the desired product. That method is called a bottom-up fabrication. Finally, nanomaterial helps increase the surface to volume ratio compared to bulk material, as easing the way for the process occurring in the surface of material such as detection and catalysis [18].

Concept of the nanotechnology was first used by Taniguchi in 1974 [20]. With EBL, fewer than 100 nm structures were fabricated. Quantum effect, which explains the physics of properties of electrons in solids by reduction of particle size, makes domination in their performances along with the thermal limitation. Therefore, such new nanoelectronic devices or nanomaterials have been advanced to solve these problems.

Richard Feynmann created the concept of nanotechnology in his lecture” There is plenty of room at the bottom “in 1959 [20]. The main idea he wants to give us is that atoms and molecules have been the possibility to be manipulated. After the invention of a scanning tunnelling microscope (STM), the year of 1981 is considered as a starting point to accelerate improvement in nanotechnology [21]. In 1986 AFM and some new materials such as carbon nanotubes were invented.

The possible nanoscale structures open a wide range of chances to discover new concepts in terms of applied and fundamental sciences. Nanostructures can be integrated into materials once conditions in which surface of structure and materials are compatible and are satisfied with their chemical compatibility or can be engineered to make functional structures. Some principles of biology, physics, and chemistry have also participated in the working area of nanostructure so that interdisciplinary relations among different departments can be improved. Nanoelectromechanical system (NEMS) achieving higher sensitivity sensors and nanobiotechnology comprised of areas of chemistry and biotechnology are few examples for a focus of interest of nanotechnology, apart from nanoelectronics applications [22].

Fabrication in nanotechnology is an assembly of bottom-up and top-down techniques. Using the top-down development, the matter is broken into the smaller basic building, whereas atoms and molecules have a tendency to arrange a complex system, called a

bottom-up approach [20]. From point of view of nanotechnology, the top-down is represented as a subtractive approach in which material is removed from the bulk material to create smaller structures. On the other hand, bottom-up deals with a combination of basic matter units to form a complex object [17]. Chemical synthesis, self-assembly, and positional assembly are the field of the bottom-up technique used to create material in the shape of particles and molecules, crystals.

Patterning, etching, and deposition are the main technique for the top-down approach to fabricate all structures. Typical tools can be arranged into two categories, one of them controlling the overall shape of the matter is with the method of etching and deposition, whereas the other that define the shape of the elements is lithographic techniques. The most commonly used types of equipment are plasma etching, reactive ion etching (RIE), evaporation, sputtering, optical lithography, EBL [20].

In the belief of nanofabrication, precision and resolution are the two important things in which are expected to under control from all outside factors. Therefore, a clean room can serve that purpose which maintains low levels of airborne particles, temperature, and relative humidity. The cleanroom is classified in terms of class, in which the maximum amount of particle is permitted per air volume [23].

## **2.2. Lithography**

Lithography was born from composite word of “lithos” which indicates in Greek as stone and graphy [24]. Alois Senefelder in Germany invented it in 1798. Lithography was a way of printing an image by using patterned color layers to papers with stone plates.

Lithography is used to fabricate patterns with specific feature sizes ranging from tens of millimetres to a few nanometers. A lot of top-down fabrication methods used in nanotechnology are derived from the semiconductor industry to fabricate various elements of the computer chip. This method is collectively named as lithography which uses a ray of light or beam of the electron. Lithography technique is combined with other

technologies such as deposition and etching so that topography can be repeated several times to form complex micro/nanostructures. Lithography technique is separated into two different types; conventional and unconventional [25]. Conventional lithography is benefitted from mask to transfer patterns on the wafer. There are different forms of masked lithography such as photolithography and nanoimprinting lithography. Unconventional lithography fabricates patterns by serial writing without the use of masks. Electron beam lithography (EBL) and focus ion beam lithography (FIB) are such types for unconventional lithography whose aims are to fabricate patterns in a serial process that permits ultra-high resolution with minimum size. In recent years lithography has been used in the nanotechnology area since it can manufacture structures in the scale of the nano dimension. In today's word all the industries are required to a smaller scale of devices because it provides benefits in terms of economics and advancements in industrial technology [26]. Making a higher breakthrough in lithography technology creates a destiny in the area of the high technology industry.

### 2.2.1. Lithographic Process

The manufacture of nanostructures requires skills to work selectively on well-defined and tiny patterns. We should define a lithographic process which covers all basic needs to fabricate them [27].

**Surface Preparation:** It is a process, which provides the cleaning and drying for the wafer surface to increase the amount of, resist adhesion to the surface called dehydration.

**Coating with Resist:** Resist, kind of polymeric film, is coated of the thin layer to provide uniform and adherent surface to the substrate to reach the desired thickness on the wafer.

**Soft Baking:** It aims to make partial evaporation of the solvent and to encourage thin resist film to adhere to the surface by reducing stresses caused by shear forces from the spinning process. Generally, for photoresist, the soft-baking temperature is in between 100C-110C.

**Exposure:** Its function is to pattern printed shapes on mask into the wafer, some amount of energy is exposed to resist as a form of irradiation.

**Development:** Based on the types of resists used in the process, it is used to remove the exposed or unexposed part.

**Hard Baking:** In addition to making soft baking, sometimes it is required to make additional solvent evaporation to improve adhesion and to increase etch resistance. The incidence of pinhole or spots in resist can be removed.

## **2.2.2. Types of Lithography**

### **2.2.2.1. Optical Lithography**

UV (ultraviolet) light is used as light sources in optical lithography. This technique depends on light-sensitive polymer (photoresist) exposed to UV light to create the desired pattern. The UV light having a specific wavelength range is illuminated through a mask that contains an opaque feature on a transparent substrate to fabricate features of the design [28]. With the help of the developer, the polymer chain of photoresist is broken down in the exposed area so that the exposed region can be more soluble in a chemical solution after inserting into developer [25]. Then, in the developer, the exposed photoresist is removed to open the area of structures if the photoresist is a positive feature. That patterned structure can be used as a protecting layer for the etching or deposition process on substrates. There are three types of patterning techniques:

#### **2.2.2.1.1. Contact Printing**

Wafer covered by photoresist is pushed against a photomask by specific pressure and UV visible light whose wavelength is between 300 and 450 nm as seen in Fig.2.1a exposes resist. The advantage of the printing is to have a resolution between 0.5-0.8  $\mu\text{m}$  [24]. However, repeated mask-wafer contacting step degrades the quality of mask and wafer by creating defects, which prevent intimate contact between wafer and mask and then diminishes resolution. Contact printing is still used in research and development (R&D). A higher resolution is not achieved due to the inability to reduce the gap between the

mask and flat surface, even when the vacuum system is used to keep the two parts together [29]. The following formula is described for resolution;

$$2b_{min} = 3\sqrt{\lambda(s + 1\left(\frac{1}{2}\right)z} \quad (2.1)$$

where

2b = grating period

s = gap width

$\lambda$  = wavelength of the exposing radiation

z = photoresist thickness

### 2.2.2.1.2. Projection Printing

Projection printing uses a dual-lens system to project a part of the mask image on the wafer surface as described in Fig. 2.1c. Mask and wafer are separated by centimetres and two lenses are used to focus the mask on the wafer surface [28]. With the help of the method, high resolution is obtained. Defects or particles on the mask are reduced significantly. The minimum feature size is related to the wavelength of light. The approximate estimate of minimum feature size F is given by

$$F=0.5 \times \frac{\lambda}{NA} \quad (2.2)$$

where  $\lambda$  is the wavelength of the light source and NA is a numerical aperture defined in terms of convergence angle  $\Theta$ .

$$NA = \sin \Theta \quad (2.3)$$

For NA = 0.5, the minimum feature size is directly related to the wavelength of the optical source. The second worry is the distance of the depth of field, DF, in which focus is kept on. Its formula is described as follows;

$$DF = 0.6 \times \left( \frac{\lambda}{(NA)^2} \right) \quad (2.4)$$

### 2.2.2.1.3. Proximity Printing

Mask is brought in very close proximity to the wafer and does not contact with wafer during the exposure but is placed with the separation of 20 to 50  $\mu\text{m}$  as shown in Fig.2.1b. Since the mask is not in contact with the wafer, diffraction limits the accuracy of pattern transfer [24]. That method leads to reduce the resolution. and helps to avoid defects of mask and wafer.

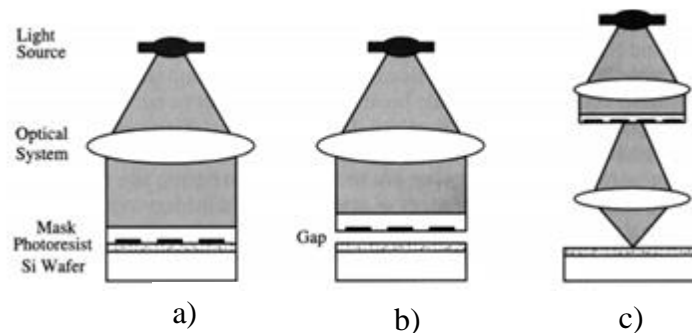


Figure 2.1 Patterning techniques; a) Contact Printing, b) Proximity Printing, c) Projection Printing [30]

### 2.2.2.2. X-Ray Lithography

X-rays are electromagnetic waves, with the wavelength in the range 0.01-10 nm and are considered as propagating as waves and interacting as photons. X-rays are produced by decaying into a core hole from higher atomic orbital, resulting in the emission of energy equivalent to the difference in the energy between two levels [31]. X-ray lithography is a more developed version of optical lithography in terms of having short wavelengths is the ability to improve resolution by reducing the diffraction effect. As a result of the short wavelength, high resolution can be obtained for the applications. Although it has a more positive effect than optical lithography, in the industry it doesn't prefer much more since new exposure dose, mask, resist and alignment should be presented, but it leads to cost increase and process risk [32].

### **2.2.2.3. Ion-Beam Projection Lithography**

Heavier ions can hit surface with much greater energy density to mill patterns such as; semiconductors, metal or ceramic substrates [33]. In EBL lithography, broadening of feature frequently is observed by scattering of a beam of electrons so that proximity effect correction can be applied to make compensation for errors [26]. However, since heavier ions such as protons ( $H^+$ ) has little scattering, the amount of backscattering is reduced. A higher resolution is formed with a focused ion beam (FIB) since the pixel size is nearly equal to the beam spot size and no exposure happens between pixels [33]. To deposit material such as tungsten, platinum via ion beam deposition, FIB systems are also performed. When a precursor gas such as tungsten hexacarbonyl  $W(CO)_6$  is released into the chamber, the focused-ion beam hits the precursor gas by causing gas decomposition leaving a non-volatile component on the surface [34,25].

### **2.2.2.4. Nanoimprinting Lithography**

With low cost, high throughput and resolution, nanoimprint lithography is a simple process. Mechanical deformation of imprint resist can create patterns. Through imprinting, the resist is cured by heat or UV light. The resolution is no longer limited by light diffraction as is the case for e-beam lithography [35]. Therefore, there is no fundamental resolution limit for nanoimprint lithography. Mold structure is the limit to determine the resolution. This technique is separated into two categories; hard and soft nanoimprint lithography which refers to the quality of the mold. Hard nanoimprint lithography operates a mask made of a rigid material such as silicon or quartz, enabling to the support of the fine structures as tiny as 5 nm [35]. Soft nanoimprint lithography recovers some challenges such as defect rates from particles and trapped air bubbles on the nonconforming substrate. Mold consists of an elastomeric material such as Poly (dimethylsiloxanes) (PDMS) [36].

## CHAPTER III

### ELECTRON BEAM LITHOGRAPHY AND IRRADIATION OF RESIST

#### 3.1. Electron Beam Lithography

The first electron beam lithography machine, based on the scanning electron microscopy, was developed in 1965 [24]. It plays an important role in improving the semiconductor industry and metal structures. When a sub-micron resolution is desired, EBL has widely used fabrication technique, especially in research and development. It has many attributes such as having high resolution, high accuracy in alignment, flexible technique working with a variety of material, but expensive and complicated systems [32].

In this method, a wafer is uniformly covered by the resist. When it is exposed to a beam of the electron, chemical structures of resist are changed. If resist is positive, the exposed area becomes solvable by using a special solvent called “Methyl isobutyl ketone (MIBK)”. If it is negative, the unexposed area is solvable as illustrated Fig.3.1. After development, resist patterns formed on the surface can serve as etch mask or lift-off layer.

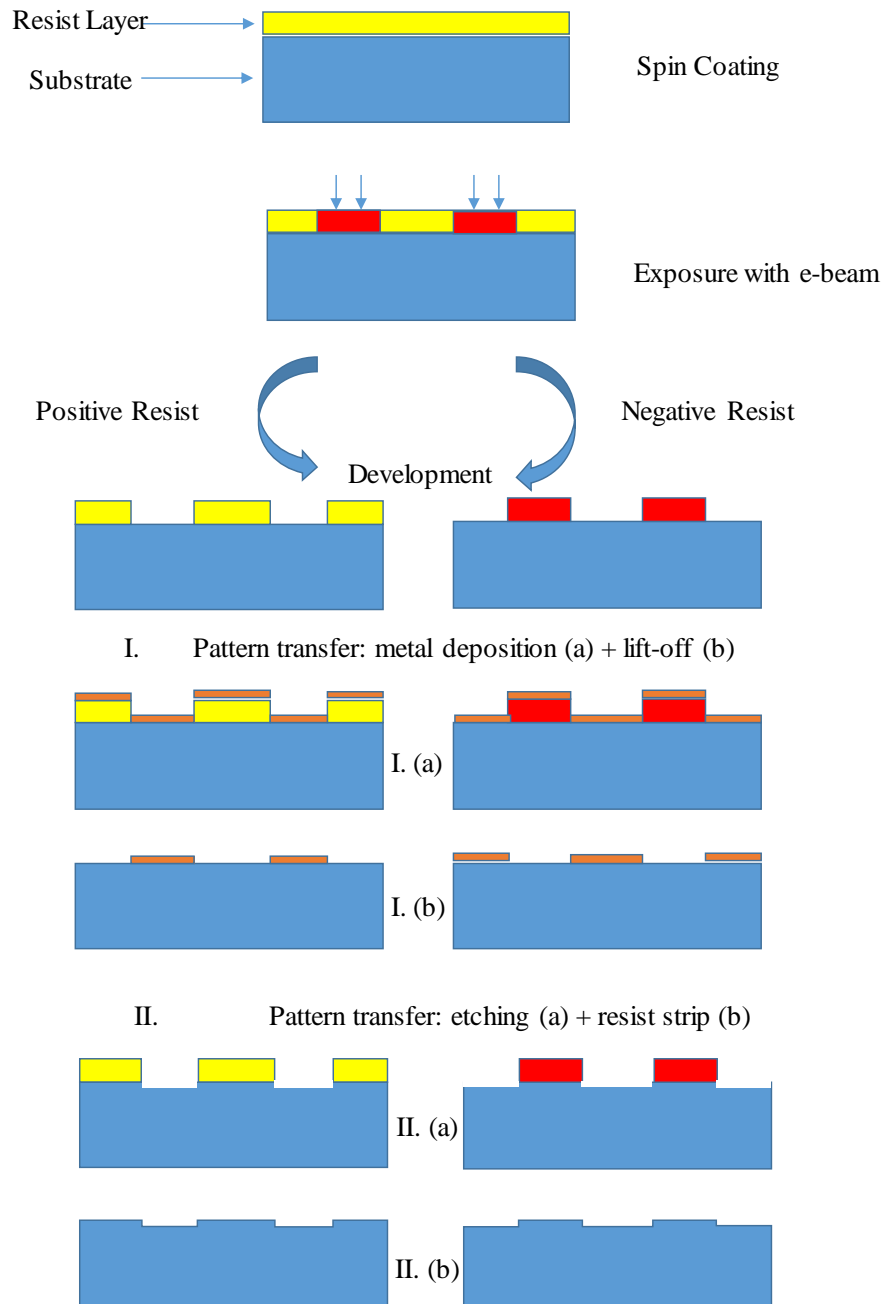


Figure 3.1 Schematic for positive and negative resists [9]

Photo-mask, typically the chrome-on-glass masks used by conventional lithography, is fabricated by EBL because it has provided high resolution, accuracy and process speed [29]. Another area is to write directly on the sample by eliminating the time-consuming mask step. Compared to optical lithography, you can get precious alignment and resolution. However, throughput (speed of writing) is lower than optical lithography.

The exposure dose is expressed as the amount of electron ( $\mu\text{C}$ ) exposed in per unit length (cm) for a single pass, or per unit area  $\text{cm}^{-2}$  for area dose [27]. The main idea for proper patterns required to achieve the desired chemical structure is to provide enough amount of energy per unit area. There are different concepts of dose for the area, lines, and dots.

$$\text{Area}_{\text{Dose}} = \frac{I_{\text{beam}} \times T_{\text{dwell}}}{s^2} \left( \frac{\mu\text{As}}{\text{cm}^2} \right) \quad (3.1)$$

$$\text{SPL}_{\text{Dose}} = \frac{I_{\text{beam}} \times T_{\text{dwell}}}{s} \left( \frac{\mu\text{As}}{\text{cm}} \right) \quad (3.2)$$

$$\text{Dot}_{\text{Dose}} = I_{\text{beam}} \times T_{\text{dwell}} \text{ (pAs)} \quad (3.3)$$

where  $I_{\text{beam}}$  is beam current,  $T_{\text{dwell}}$  is pixel dwell time and  $s$  is the step size.

Some other parameters should be decided carefully to make the process of exposing the patterns. Spot size or beam diameter is the physical width of the electron beam during the pattern writing and is set by beam current. Step-size or resolution is the distance between the spots of the focused electron beam. To minimize the proximity effect, the step size, at least, should be equal to half of the spot size [27]. There are three possibilities in the relation of the beam and pixel size. Their relation can be described in Fig. 3.2. In Table 3.1, the theoretical spot size at 100 kV for Vistec EBL lithography is illustrated at an aperture of 300  $\mu\text{m}$ .

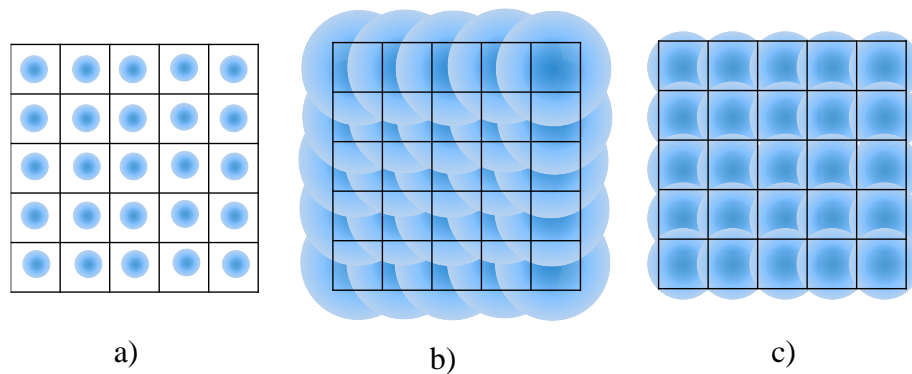


Figure 3.2 Relation of the beam and pixel size; a) Beamwidth too small for pixel width, pattern not fully exposed, b) Beamwidth too large for pixel width, pattern washed out, c) Good pixel/beam size ratio, the pattern is evenly exposed <sup>1</sup>

<sup>1</sup> [http://apps.mnc.umn.edu/archive/ebpgwiki/rsrc/EBPG/SoftwareTraining/EBPG\\_Training.pptx](http://apps.mnc.umn.edu/archive/ebpgwiki/rsrc/EBPG/SoftwareTraining/EBPG_Training.pptx)

Table 3.1 Theoretical Spot Size for 100 kV<sup>1</sup>

Beam current (nA)	Spot Size for 300 $\mu\text{m}$ aperture (nm)
0.1	5
0.5	5
1	5
5	5
10	16
50	40
100	60

### 3.2 Electron Beam Resist

In this section, standard e-beam resist types are presented. There are two types of resist: inorganic and organic. The main difference in EBL is that the primary beam only affects inorganic resist, whereas secondary and backscattering electrons can modify organic resist. Inorganic resist shows higher resolution, but lower sensitivity and challenges to combining the subsequent fabrication process.

General procedure for resist application can explain as follows; wafer is coated with a liquid resist consisting of polymer, photoactive component, and solvent, and then spun at 1000 to 6000 rpm to form a uniform coating onto wafer [32]. After baking for casting solvent, electron exposure affects the chemical structure of the resist, leaving it either more soluble (positive) or less soluble (negative) in the developer as shown in Fig.3.1. After the electron beam exposures the chemical structure of positive resists, it leads to polymer chain scission so that polymer chain length is reduced; therefore, the exposed area in the resist is more easily dissolved in the developer than the unexposed resist. Either the pattern is formed to substrate by through etching process or “lift-off” of material as described in Fig. 3.1. There are two types of EBL resist: positive and negative. Popular e-beam resist, and their properties are listed in Table 3.2.

Having wider process latitude is related to have an ability of higher contrast for resist. To be affected by proximity effect very less, resist should be exposed or developed as much less as possible but, resist is cleared down to the bottom for all patterns [32]. The usage of e-beam lithography is to reach high resolution and sensitivity. However, reaching the two aims at the same time usually is not possible since resist has a limit for sensitivity. The minimum feature size or distance between the two patterns resolved is defined as resolution. The limiting factor for resolution is attributed to relations between resist molecule and incoming electrons and to the range of scattering electrons. Establishing exact value is often difficult, so it is considered that features of few nanometers can be fabricated with EBL more controllably and repeatedly. To achieve selective development, the minimum dose is required. Sensitivity quantifies that amount of delivered dose. Since higher sensitivity allows fast writing, it is always desirable. Contrast is explained abrupt changes of thickness on the dose, which has also influence on the resolution. It is found from the linear slope of the sensitivity curve;

$$\text{Contrast} = \frac{1}{(\log D - \log D^0)} = \left[ \text{Log} \frac{D}{D^0} \right]^{-1} \quad (3.4)$$

where  $D$  is the dose of complete development and  $D^0$  is the dose which leads to no resist dissolution on the developer.

To obtain very high resolution, high acceleration voltage, which is between 50 and 100 keV, are preferred. This is because, with the increase of beam energy which dose should be higher, the accumulative energy deposition in the resist has decreased which is consistent with a theory explaining that energy loss of electrons per unit path length and scattering decreases with beam energy, indicating better throughput of low energy [37]. However, backscattered electrons returning from the substrate lead to exposure of areas close to the intended pattern. On the other side, at low acceleration voltage, which is between 2 and 20 keV, the penetration depth is not more and so most of all energy in the resist layer will be lost. It implies that the exposure efficiency and sensitivity or throughput of lithography tool are increased, but it causes problem of high resolution by increasing lateral spread within resist film [38]. Proximity effect is reduced because of

the minimization of electron scattering from the substrate. However, using a low acceleration voltage, you have a disadvantage which is to increase in the beam size. Hence, it is necessary to use thin layers. In the case of a thick layer, it is not possible to expose all parts of resist.

### **3.2.1 Charge Dissipation**

Charge dissipation is a more frequent problem for insulating substrates during exposure of resist and leads to significant distortion during the patterning [12]. One of the basic solutions is to evaporate a thin layer of gold, gold-palladium alloys, chrome on the top of the resist. That method is likely to reduce the possibility of scattering during exposure. Before developing a process, they can be removed by using a related metal etchant. E-beam evaporation should not be selected for metal evaporation since x-rays produced by electrons in the evaporators expose the resist randomly. Another approach to eliminating charge dissipation is to either use of a conducting polymer under or top of the resist instead of evaporation thin metal layer on the resist.

### **3.2.2 Positive Resist**

Positive tone resist is based on the removal of exposed resist material. During exposure, the secondary electron from inelastic collision changes the chemical composition by chain scission, called polymer fragmentation. As a result, the solubility of patterned features is increased when immersed in the developer. After exposure, resist profile can be controlled by manipulating the value of exposure dose and development time or developer types [39]. Fig.3.3 shows a possible edge profile for positive resist.

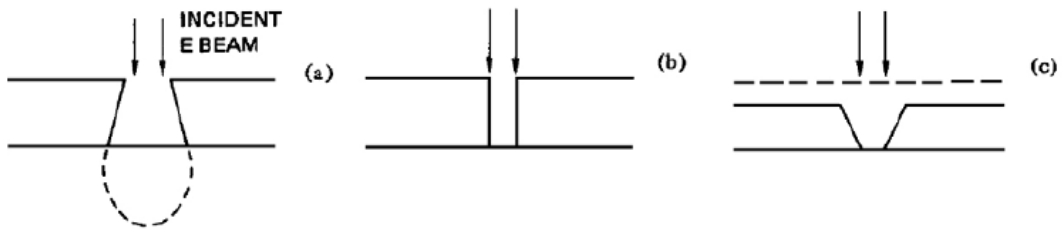


Figure 3.3 Edge profile in positive resist [39]

### 3.2.2.1 PMMA

PMMA primarily is used and available at different compositions, concentrations, and weight. PMMA can be solved in different solvents like anisole, chlorobenzene. The concentration rate determines the viscosity of PMMA. The thickness of resist depends on the concentration and spin-speed. PMMA is usually available for two kinds of weight form, 495 and 950K MW, in casting solvents such as chlorobenzene and anisole. The substrate is coated with PMMA and baked at 170 °C to 200 °C. Electron exposure breaks the polymer into fragments as seen in Fig.3.4 that is dissolved by the developer such as MIBK, which is a stronger developer. Therefore, to protect some of the unexposed regions, the developer is usually diluted by mixing in a weaker nonsolvent such as IPA. In the positive mode, PMMA has a high resolution [32]. If selected dose value is more than a nominal dose for positive resist, PMMA will crosslink of the polymer molecules, forming a negative resist. PMMA is generally preferred for EBL due to providing high resolution with ease of the process and low cost [36]. Compared to novolac-based photoresist, PMMA has poor resistance to plasma etching.

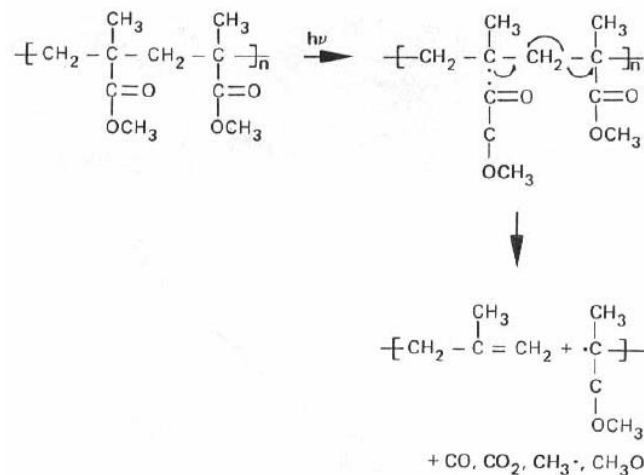


Figure 3.4 PMMA reaction mechanism [24]

### 3.2.2.2 EBR-9

Compared to PMMA, this resist is evaluated to display faster development rates due to its higher sensitivity to e-beam exposure dose; however, the trade-off is in lower resolution [31].

### 3.2.2.3 PBS

It is widely used to mask plate patterning. For the production of high volume mask, sensitivity is very high which provides an advantage from all other positive resists, higher exposure throughput [24].

### 3.2.2.4 ZEP

ZEP contains copolymer of chloromethacrylate and methylstyrene [40]. In terms of sensitivity, it is faster than PMMA. Unlike EBR-9, the resolution of ZEP is close to PMMA. The etch resistance of ZEP in fluor based gas is better than PMMA [24, 32]. However, the price is high, and it is also hard to view resist line under SEM.

### 3.2.2.5 Copolymer

Copolymer resists are based on a mixture of PMMA and some “ratio” of methacrylic acid which is otherwise known as MMA (“ratio”) and used widely in EBL. To perform the bi-layer lift-off resist process, it is used with PMMA [41]. A copolymer is expensive than PMMA.

### 3.2.3 Negative Resist

Negative resist works by cross-linking the polymer chains together, resulting in a resist layer, which is less soluble in the developer after exposure to radiation .and the unexposed area can be removed by the developer solution. However, there are some problems with swelling during the development and bridging between features. Controlling over resist profile for negative resist is not easy compared to positive resist. In negative resist, the edge profile of line after exposure looks like bell-shaped as illustrated in Fig.3.5 [39].

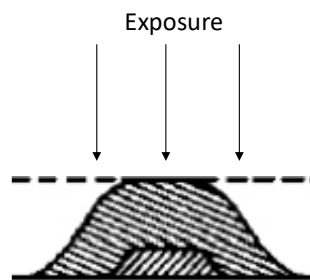


Figure 3.5 Negative profile after exposure [39]

#### 3.2.3.1 COP

It is an epoxy copolymer of glycidyl methacrylate and ethyl acrylate. It is used for negative exposure of mask plates. Sensitivity is very high, but the resolution is relatively poor [32].

### 3.2.3.2 HSQ

It is a type of inorganic resist. Compared to organic resist like PMMA, HSQ shows higher contrast and higher etch resistance, but lower sensitivity[42]. Since their chemical structure is changed under the e-beam irradiation, it leads to variations in the dissolution rate during the development process.

Table 3.2 Comparison of commercially available electron beam resists [24,36]

<b>Resist</b>	<b>Tone</b>	<b>Sensitivity (<math>\mu\text{C}/\text{cm}^{-2}</math>)</b>	<b>Developer</b>
PMMA (HMW)	Positive	900 at 100kV	MIBK:IPA
PMMA. (LMW)	Positive	800 at 100kV	MIBK:IPA
Copolymer	Positive	300 at 100kV	MIBK:IPA
ZEP520	Positive	300 at 100kV	Xylene:Pdioxane
EBR-9	Positive	10 at 100 kV	MIBK:IPA
PBS	Positive	1 at 100 kV	MIAK:2- Pentanone 3:1
HSQ	Negative	1000 at 100kV	TMAH

### 3.3 Parts of E-Beam Lithography Machine

The electron beam is formed at the electrical optical column, which is the part of the EBL system. An EBL column includes an electron source, two or more lenses, a blanker, a stigmator, apertures, alignment system and electron detector as seen in Fig.3. 6. Required energy for acceleration occurs in the region between the cathode and the anode. The reason for occurring on all things in the column of EBL under a high vacuum is to prevent the electron's trajectory from being influenced by the electrons' collision against gas molecules.

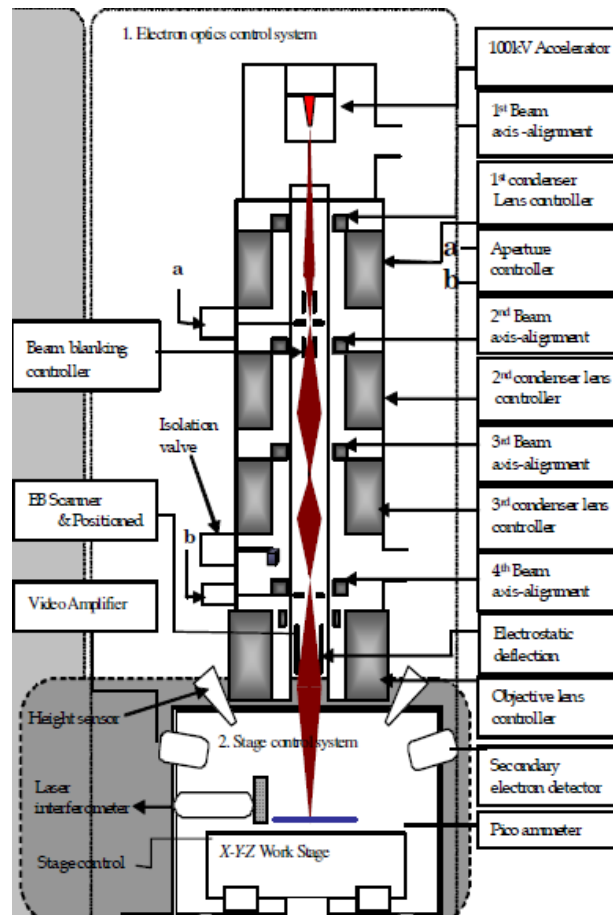


Figure 3.6 Block diagram representing basic components of typical electron beam lithography [11]

### 3.3.1. E-Beam Lithography Column

#### 3.3.1.1 Electron Gun

Electrons that have enough energy to overcome the work function barrier of conductors are emitted by a conducting material either heating it to the point or applying the electric field sufficiently [10]. There are three key parameters for the sources: virtual source size for determining the amount of demagnification, its brightness for representing the amount of current and the energy spread of the emitted electrons. The thermionic source is illustrated in Fig.3.7, which the beam generated by heating materials is not very bright and has a large energy spread, and shorter lifetime because of the high operating temperature. Field emission source which electron is emitted from sharp tips of material

by applying high electric fields due to sharp tip, but it has instability in terms of short-term noise because of atoms leading to adsorb onto the surface tips. Since the source of thermionic field emission is the combination of both field emission and thermic source, it is the best source due to having features of less sensitive to environmental conditions and longer life expectancy. For high resolution, the size of the source and bandwidth of emission energy may be small. In the case of smaller virtual size, you have a smaller beam spot on the sample. Table 3.3 shows different types of electron guns.

Table 3.3 Type of electron guns [24]

Source Type	Brightness ( $A/cm^2/sr$ )	Source Size	Energy Spread (eV)	Vacuum Requirements (Torr)
Tungsten Thermionic	$\sim 10^5$	$\sim 25 \mu m$	2-3	$10^{-8}$
$LaB_6$	$\sim 10^6$	$\sim 10 \mu m$	2-3	$10^{-8}$
Thermal FE	$\sim 10^8$	$\sim 20 \mu m$	0.9	$10^{-9}$
Cold FE	$\sim 10^9$	5 nm	0.22	$10^{-10}$

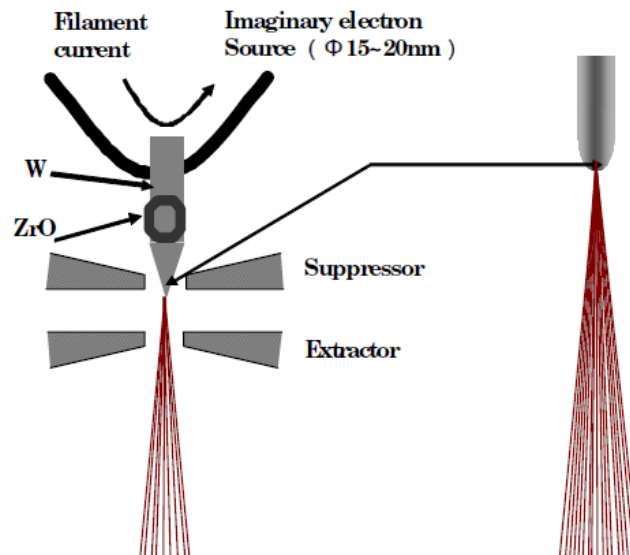


Figure 3.7 Electron gun with a thermal field emission gun [11].

### **3.3.1.2 Electron Lens**

With the help of either electrostatic or magnetic forces, electrons can be focused. Electron lenses are made only to converge which means that travelling of the beam of electrons is parallel to its principal axis. Aberrations are critical to EBL. Spherical aberration means that the inner zone has a less tendency for strongly focusing than outer, and so the beam of electrons does not converge at the same point after passing through the lens. Chromatic aberration that is based on different energies atoms is focused on different image planes. To minimize both kinds of aberrations, the convergence angle is reduced. In this manner, although electrons are restricted to the center of the lenses, it leads to reduce the amount of beam current [40]. Since electrostatic lenses have worsened aberration than a magnetic lens, so they are placed in the gun region as a condenser lens. Magnetic lenses are preferred to focus the beam more than electrostatic lenses.

### **3.3.1.3 Aperture**

The beam passes on small holes down the column. Stopping any stray electrons is provided with the aperture without affecting the beam itself. Aperture controls the beam convergence angle in which electrons can pass through the system. It also controls the effect of lens aberrations and sets the beam current [40].

### **3.3.1.4 Beam Blanking**

Pair of plates arranged as a simple detector can help the beam turning on or off successfully. It prevents electrons from reaching the sample surface [24].

### **3.3.1.5 Stigmator**

It is used to correct for imperfections in the construction and alignment from EBL so that astigmatism can be removed. Then, the beam is returned to normal shape. Stigmator system is responsible for correcting the beam shape as being circular again.

### 3.3.1.6 Electron Beam Deflection

Electron beam deflector as described in Fig.3.9 achieves scanning the beam across the surface. Aberrations which lead to beam diameter to deteriorate and deflection in X and Y direction are introduced by the deflection of the beam off-axis. Electron deflector can control the deflection angle of the beam in which determine positional accuracy of exposure pattern. The system contains a two-tier deflector to reduce any aberration of the axis of the beam [11]. There are two types of scanning methods, one of which is vector-scan, Fig.3.8a, in which the beam is deflected only over the entities to be exposed. The other is raster-scan, Fig.3.8b, in which the beam scans all the entries at a constant speed [11].

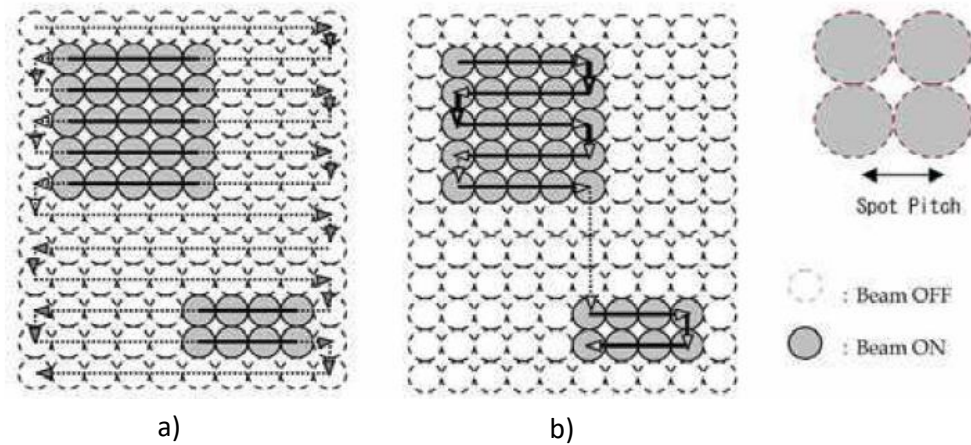


Figure 3.8 Scanning methodologies for the beam of the electron: a) raster scan and b) vector scan [11]

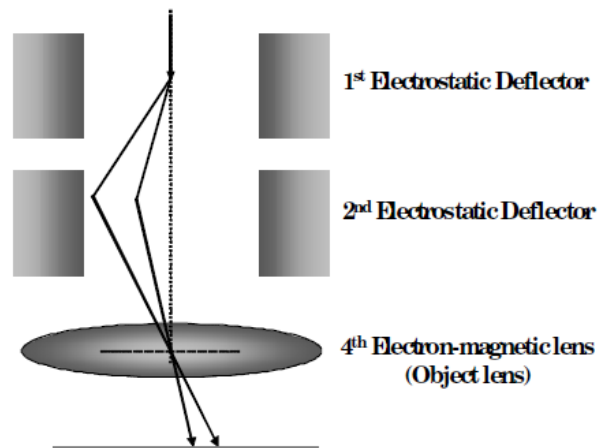


Figure 3.9 Schematic drawing of electrostatic deflectors [11]

### 3.3.1.7 Beam Axis Alignment Coil

The deviation between lenses is corrected by beam axis alignment. 4 sets of alignment coil are placed immediately above each of the four electromagnetic lenses. Two coils generating a horizontal magnetic field in the X-Y plane creates an alignment as shown in Fig. 3.10.

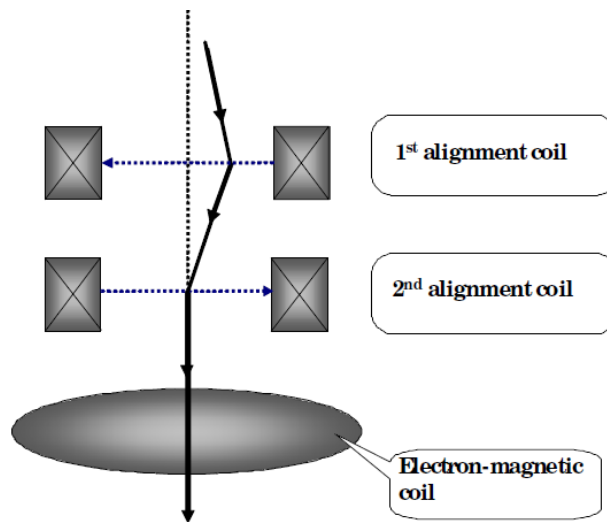


Figure 3.10 Schematic drawing of beam axis-alignment coils [11].

### 3.3.2. Mechanical System

Mask or wafer stage and loading system are included in the mechanical system. Chamber is equipped with a CDD (charge couples device) camera to make visualization inside the chamber and to control positioning

### 3.3.3 Vacuum System

Performance of the vacuum system improves beam performance and resolution. Different types of gun source can specify amount of vacuum value.

### **3.3.4 Computer**

To transfer pattern information for the generation of the data file, a computer is used to create an interface with a machine to control the mechanical system and electron optical column.

## **3.4 Terminology**

To prevent confusion, it is necessary to define some terminologies used in the EBL. The reader can have enough idea about EBL jargon.

### **3.4.1 Writing Field**

It is the largest area covered by electron-beam deflection without the stage moving and its size, ranging from few tens of microns to few millimeters [43], is decided by the magnification of the microscope

### **3.4.2 Stitching**

Due to pattern dimensions, if exposure needs more than one writing field, the field is stitched together via stage movements. It is known that the field edges align with each other.

### **3.4.3 Exposure Element**

Each writing field is divided into a set number of exposure elements (EXELs), which are decided by specific main Digital to Analog converter (DAC) placed on tool; so smaller fields permit better definition of finer features [27]. With DAC of 4 bits, the deflection in

one dimension permits to define 16 different positions. Each value determines a pixel. Therefore, to write a line, the beam is turned into on, begins to deflect at determined speed until the end, and switched off. On the other hand, in the two-dimensional system, it is more complicated [20].

#### **3.4.4 Exposure Dosage**

It is the amount of energy deposited per unit area. It is measured in terms of current deposited per unit area,  $\mu\text{C cm}^2$ . The dosage depends on the type of resist and dimension of patterns written.

#### **3.4.5 System Clock**

It is called as writing speed. It is inverse of dwell time of beam. The higher clock means to faster exposure.

#### **3.4.6 Proximity Effect**

Since the different types of scatterings such as elastic and inelastic are undergone by electrons in the substrate, the amount of energy is deposited away from the desired area, resulting in unwanted features or geometries after development. Using advanced software can correct proximity effects.

#### **3.4.7 Beam Current**

It identifies the amount of electron hitting on the sample for each second. Due to charge density, its value affects the highest resolution. High current can create physically larger structures than the small current one.

### 3.5 Conceptual Flow

Some of the basic things used in the EBL are demonstrated in Fig.3.11. Each of them will be explained below;

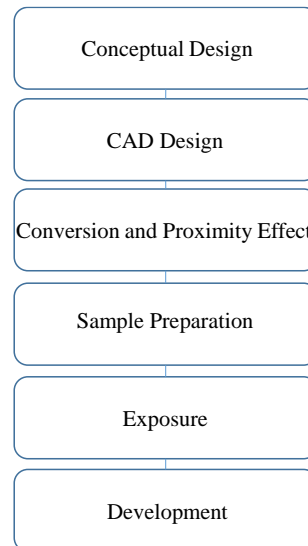


Figure 3.11 Diagram for some of the basic things for EBL

#### 3.5.1 Conceptual Design

The final device should be finalized in your mind before starting any process in the fabrication step. It is critical to define proper final geometry and to decide important dimensions of the final device. By the means of the final layout, specifications for related writing field and beam current are determined. Additionally, in terms of all steps for fabricating the final device, making a clear layout can facilitate the choice of resist type, dosage and so on.

#### 3.5.2 CAD Design

The pattern exposed is designed with the help of a suitable layout package. GDSII file is an acceptable file for such a design to continue the rest of the process. [27].

### **3.5.3 Conversion and Proximity Effect**

It is necessary to translate a GDSII file into a machine-exposable file containing all details needed by pattern generators to scan the beam. Shapes are fractured to be exposed to trapezoid before exposure. After that, a trapezoid is divided into pixels. Proximity effect is not always required and depends on the operator's desired whether composition for proximity effect is needed or not. However, to correct proximity effect, the software is performed by correcting the exposure dosage based on the physical model executed into it [27].

### **3.5.4 Sample Preparation**

EBL has a limited depth of focus and so, flat surface is preferable for EBL, leading to being perpendicular to the incoming beam. However, some systems can permit the surface of sample height correction measured by a laser beam. Basic sample preparation is described below;

- Cleaning substrates with acetone by the help of sonication
- Rinse in clean acetone quickly and IPA
- Blow dry under nitrogen
- Resist deposition and bake

The selection of resist should be made in the conceptual design phase to satisfy the requirements of fabrication steps. Electrical grounding is required to avoid charging effect resulting in loss of pattern accuracy. If an insulating substrate is used as a substrate, 5-10 nm thick of Cr, Al, or Au can be deposited either between the substrate and the resist or on top of resist. Then, it is arranged on the sample holder and transferred into the vacuum chamber to be exposed.

### **3.5.5 Exposure**

Job file is a program for exposure whose aim is to allow writing for a long time without interfering in the operator process. Stage automatically is moved in the required positions. It means that each trapezoid is written by deflecting the beam to each pixel. By the Gaussian intensity profile, the sub-element that is created by the original design is continuously exposed. For each sub-element, the beam is switched off and it turns to the next fragment. The positioning system by the laser interferometric stage is suitable to optimize the stitching prevision.

### **3.5.6 Development**

To remove the exposed resist, the development process is critical for controlling precise features. Ultrasonic agitation can be useful during development but once being a decision, this must be considered whether the other parameters are affected or not.

## **3.6 Electron-Solid Interaction**

As a result of the penetration of electrons into the resist, they experience many small-angle scattering events, causing broaden for initial beam diameter. When electrons penetrate through the resist into the substrate, they experience large scale scattering events [44]. Proximity effect is occurred by backscatter scattering and affects the amount of dose which pattern feature receives.

### 3.6.1 Forward Scattering

When the electrons penetrate the resist, many of them experience small-angle scattering in resist, which results in a broader beam profile. The increase of beam diameter due to forward scattering can be defined as follows;

$$d_f = 0.9 * \left(\frac{R_f}{V_b}\right)^{1.5} \quad (3.5)$$

where  $d_f$  is beam diameter,  $R_f$  is resist thickness and  $V_b$  is beam voltage in kV.

According to formula, forward scattering can be minimized by increasing more beam voltage or decreasing the resist thickness. Although you take some precautions to prevent forward scattering, it should be considered that the resist sidewall profile will be changed from a positive slope to a negative profile by the help of forward scattering to get positive acquisitions for lift-off [21].

### 3.6.2 Backscattering

Large angle scattering is experienced when electrons do not stop to penetrate through resist into the substrate [44]. Many of them might return through resist far from incident beam by resulting in additional resist exposure.

### 3.6.3 Secondary Electrons

Form of the secondary electron is created by dissipating much of the energy of forward scattering electrons without changing its direction [32]. They have responsibility for the bulk of the actual resist exposure process. Their mean free path is around 1 nm [38]. Therefore, their distribution is dependent on the trajectory of the primary beam.

### 3.7 Proximity Effect

The dose given by the EBL tool is not applied efficiently to the shapes since line variation has occurred; it is known as the proximity effect [45]. A type of lines placed between two large area may receive many scattered electrons which result in developing more, whereas small isolated features whose width is much smaller than the pitch, may receive less dose compared to larger or densely areas [32]. When resist is bombarded by the electron, most of the electrons attempt to scatter with small-angle forward scattering, leading to widening the primary beam size. As the electrons penetrate through resist into the substrate, many of them undergo large-angle scattering events, resulting in backscattering, by returning to spot place in a resist where the primary beam entered. Fig.3.12 shows us the behaviour of backscattering and forward scattering.

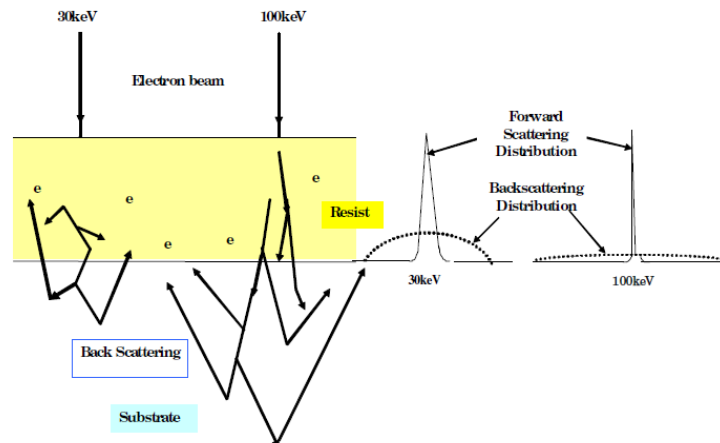


Figure 3.12 Schematic drawing for demonstrating the electron scattering for 30 keV and 100 keV on a silicon substrate [11].

### 3.7.1 Ways to Protection of Proximity Effect

- If a pattern has uniform linewidth, all required things may be adjusted the overall dose until optimum linewidth is reached. Dose modulation is the most used technique so that dose exposure values can be scaled up or down for some parts of your patterns
- If acceleration voltage is increased more as seen in Fig.3.12, it can minimize forward scattering despite fact that backscattering is getting deeper and wider. However, secondary electrons returning to the resist from the substrate have energies that are lower than breakdown energy for breaking the polymers in the resist [8].
- In the case of lower beam energy, since the electron range is smaller than the minimum feature size, the proximity effect can be reduced.
- The substrate is also critical when a substrate having a low atomic number is used, it can produce less backscattered electrons
- Resist having the capability of higher contrast can be used to minimize the linewidth variations.
- The proximity correction algorithm [45] which is important to stimulate the influence of proximity effect can be used. In that program, for each pixel, the required dose is determined with proper accuracy computationally as shown in Fig 3.13. A lower dose is used in the dense region, whereas a higher dose is preferred in an isolated region.

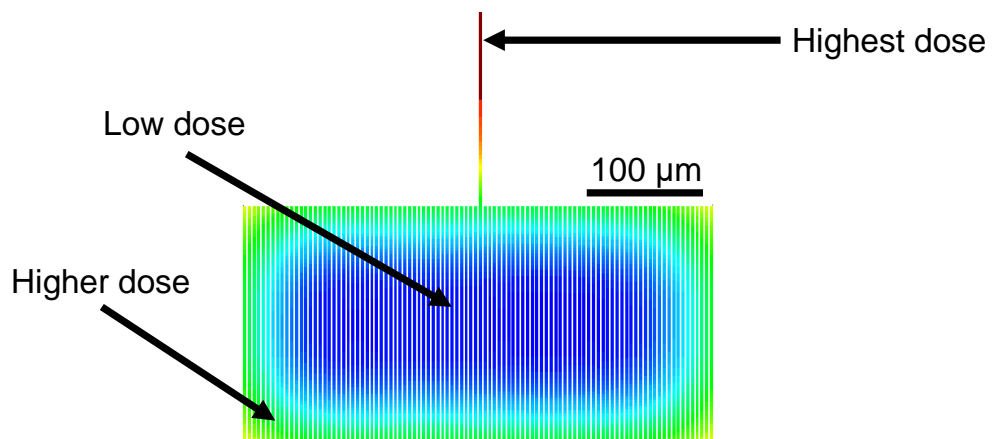


Figure 3.13 Simulation of Proximity Correction Algorithm<sup>2</sup>

<sup>2</sup> [http://apps.mnc.umn.edu/archive/ebpgwiki/rsrc/EBPG/SoftwareTraining/EBPG\\_Training.pptx](http://apps.mnc.umn.edu/archive/ebpgwiki/rsrc/EBPG/SoftwareTraining/EBPG_Training.pptx)

### **3.8 Multilayer Systems**

Multilayer resists are beneficial for lifting off metal, reducing the proximity effect and high resolution. There are many different types of multilayer systems:

#### **3.8.1 Low/High Molecular Weight PMMA**

High molecular weight PMMA is spun on top of a low molecular weight PMMA. The sensitivity of low molecular PMMA is higher than the top layer, so the resist is developed to create an advanced undercut. However, at high energy and thin PMMA, it is hard to produce an undercut profile since a straight resist profile is produced due to preventing forward electron beam exposure [11] and so the resist profile is perpendicular to the substrate. For densely packed features, an undercut profile is useful when lift-off is required. Fig.3.14a describes the resist profile for bilayer PMMA after exposure. In terms of cost-efficiency, the bilayer PMMA/PMMA is suitable to be chosen.

#### **3.8.2 PMMA/Copolymer**

To lift-off thicker metal layers, a larger undercut is usually required. In this technique, copolymer, methyl methacrylate and methacrylic acid [P(MMA-MAA)], is highly sensitive and is spun under PMMA. Polar solvents such as alcohols and ethers make soluble the exposed copolymer, but insoluble in a nonpolar solvent such as chlorobenzene. PMMA is spun on top of the copolymer. Fig.3.14b, 14c, and 14d show the relation between PMMA and copolymer for the lift-off process.

### 3.8.3 Trilayer System

In addition to PMMA/copolymer, if another PMMA is spun on top of PMMA, we have structures looking like mushroom shape. In this technique, the central line is exposed to heavy dose and a lighter dose is given to the sides [11].

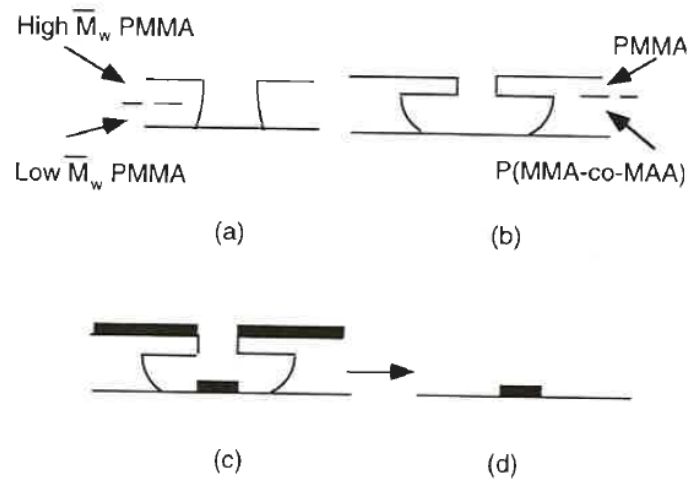


Figure 3.14 Two bilayer e-beam resist structure a) High MW PMMA / Low MW PMMA b) PMMA /Copolymer c) The resist is then removed in the solvent. d) Final structure after dissolving resist [32].

## CHAPTER IV

### RELATED WORKS

A method was found for fabricating sub-10 nm gaps [46]. Overlapping and overexposure are the basis for the study to fabricate sub-10 nm electrode gaps. The fabrication efficient was reached approximately % 100 for 8-9 nm gaps. However, for 3-4 nm gaps, the yields were reduced to almost % 15. One of the results for the study is that Fig.4.1a represents that when the amount of dose value is increased by keeping development time the same, the real interwire gap is getting narrower. On the other side, as developing time is increased gradually, the length of the gap between electrodes is increasingly narrower as shown in Fig.4.1b. As a fabrication strategy, they were benefitted from top-down fabrication by using electron beam lithography (EBL) as a lithography tool on PMMA coated on  $SiO_2(150\text{ nm})/Si\text{-boron}$  doped substrate and hot acetone ( $90^\circ\text{C}$ ) to take place lift- off condition.

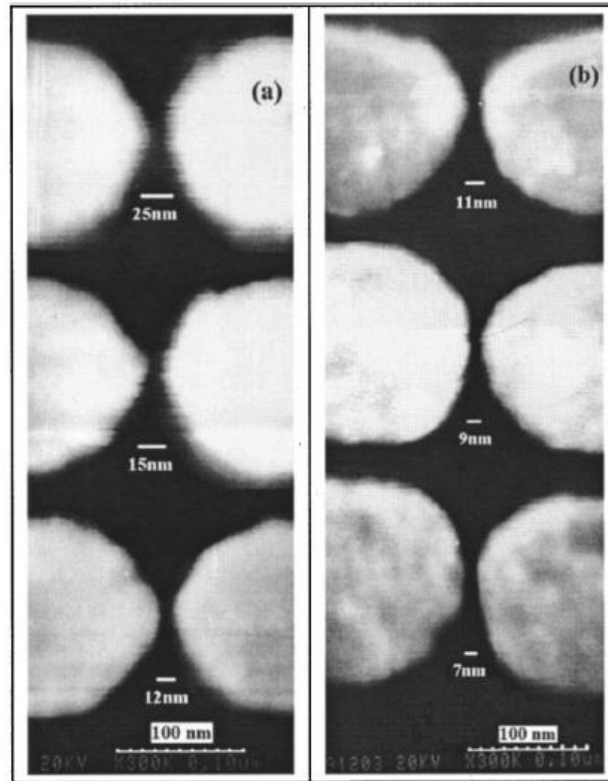


Figure 4.1 a) SEM images of the gaps using different electron doses 210, 220, and 230  $mC/cm^2$ , but same developing time of 60 s b) SEM of the gaps using different developing time doses 80, 120 and 180 s, but same electron doses 230  $mC/cm^2$  from top to bottom [46]

The bilayer of PMMA and copolymer P (MMA 8.5 MAA) as a negative tone resist was performed for the lift-off process [47]. Note that although these two resist were used as positive tone resist, overexposing caused change their chemical from positive to negative resist by inducing cross-linking of the polymer molecules, removing only unexposed regions by the developer. It is also shown that an undercut profile is crucial to succeed a proper removal of resist material along with the metallic layer during the lift-off step as illustrated in Fig.4.2. The process tries to explain how to implement a nanofabrication method of high resolution for lift-off mechanism in terms of selection of bilayer of available PMMA / P(MMA 8.5 MAA) due to show different effects towards relative height and width as a function of exposure dose.

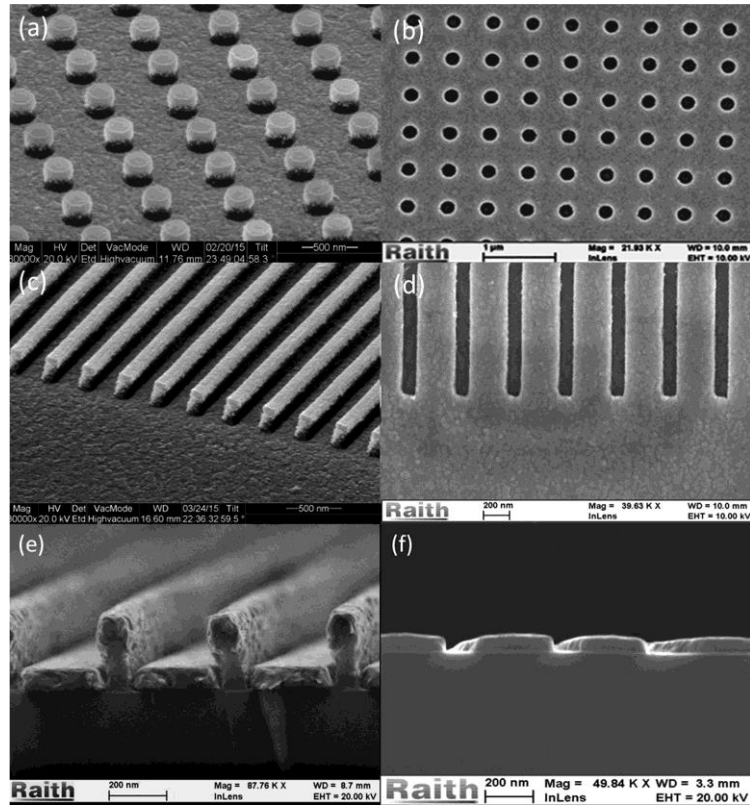


Figure 4.2 a) Nanohole array and c) Undercut profile for Nanoslit array after metal deposition b) and d) After lift-off for nanoholes and nanoslits. (e) and (f) Before and after lift-off cross-section view of the nanoslits configuration. Wide of the split is 100 nm wide, 100 nm thick; the pitch of split is 400 nm apart [47].

Nuzaihan, M et al. [48] used a top-down approach to develop silicon nanowires from silicon-on-insulator (SOI) wafers. For that purpose, e-beam lithography involved the fabrication process by characteristics of negative e-beam resist, ma-N2400. After that, to achieve wires, which are 20 nm in width and 30 nm in height, inductively coupled plasma-reactive ion etching (ICP-RIE) was used for anisotropic etch profile of silicon. To reduce the width of a silicon nanowire, silicon nanowires were oxidized in dry  $O_2$  the environment at 1000 °C for 10-20 minutes, oxidized silicon nanowire was dipped in a buffered oxide etch (BOE) to remove  $SiO_2$  layer.

Rahman, S et al. [8] described the development of silicon nanowire by using a silicon-on-insulator (SOI) as starting material, and then the nanowires were fabricated using a top-down approach which EBL method. The width of the smallest dimension was 65 nm depending on selected dose values. The fabricated device was performed as pH level detection. It is observed that smaller dimension nanowire is more sensitive because of high surface to volume ration.

Oh, Seung et al. [49] experimented to see the effect of low-voltage and high voltage EBL and to observe the influence of a lot of parameters such as acceleration voltage, aperture size, resist thickness, and baking temperature as seen in Fig.4.3. During the process, all experiments were performed on cleaned  $\text{SiO}_2$  the substrate which was coated by positive tone resist PMMA 495 K MW. The effect of acceleration voltage demonstrates that the scattering effect is more important in high-voltage EBL. The variation of width was slight at 1V than at 10V. Additionally, it is believed that the scattering angle of the resist increases with the thickness. To examine the characteristic feature of aperture size, the different size of the aperture was performed. Aim of aperture size is to set the angle of beam convergence in which electrons can pass through the e-beam system, to control beam current and the effect of lens aberrations. After observations, at low acceleration voltage, aperture size significantly affected exposed patterns, but at high acceleration, since acceleration voltage provided high energy, the effect of diffraction was small. In the case of the effect of various baking temperatures, at low temperature, the width of the exposed line is larger than at high baking temperature because of the relatively low linking of the polymer chain.

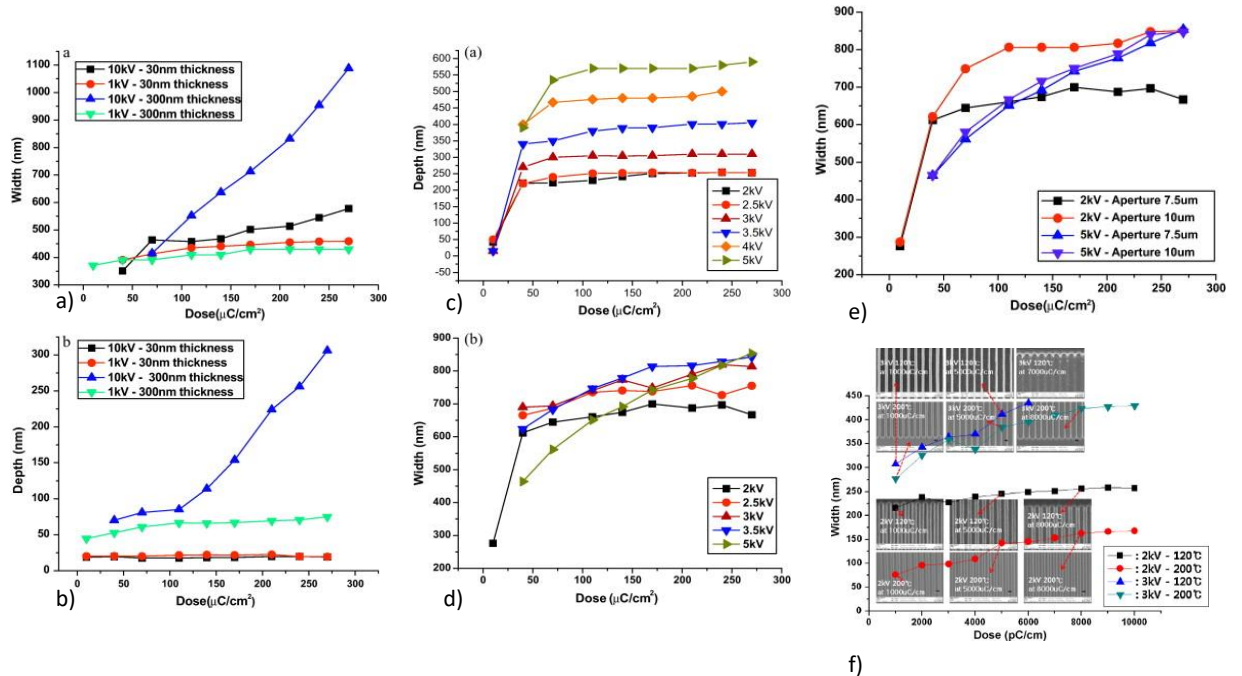


Figure 4.3 Features of exposed patterns: (a) width and (b) depth for low- and high-voltage EBL for 1 and 10 kV and resist thicknesses for 30 nm and 300 nm, c) depth and d) width for acceleration voltages of up to 5 kV and resist thickness of 600 nm, e) various aperture sizes for 2 kV and 5kV, f) various baking temperatures [49].

Humaira et al. [50] fabricated 40 nm silicon nanogap on silicon on insulator (SOI) wafer by using electron beam lithography (EBL). The process started with coating by ZEP 520, positive e-beam resist, and after some fabrication steps, in the last step by making dry etching process; final nanogap pattern was obtained after removal of resist mask. The next method was to fabricate the gold electrode on top of nanogap using the photolithography. Titanium and gold were deposited to the substrate and then after making related photolithography step by mask, final gold electrode patterns were obtained by the wet metal etching process of titanium and gold layer and then removing the photoresist.

Vieu, C et al [51] tried to find a resolution limit for conventional polymethyl methacrylate (PMMA) organic resist. In that work, the resolution limit was tried to push below 10 nm for isolated features and a dense array of periodic structures was fabricated at a pitch of 30 nm as illustrated in Fig.4.4. Development of resist and pattern transfer is limiting factors for resolution after exposure. With their method, fabrication of sub-10 nm lines by the lift-off and 30 nm pitch array by lift-off and reactive ion etching (RIE) were optimized for making them reproducible. Additionally, the development of resist using ultrasonic agitation in pure IPA provides advantaged in obtaining very dense arrays easier.

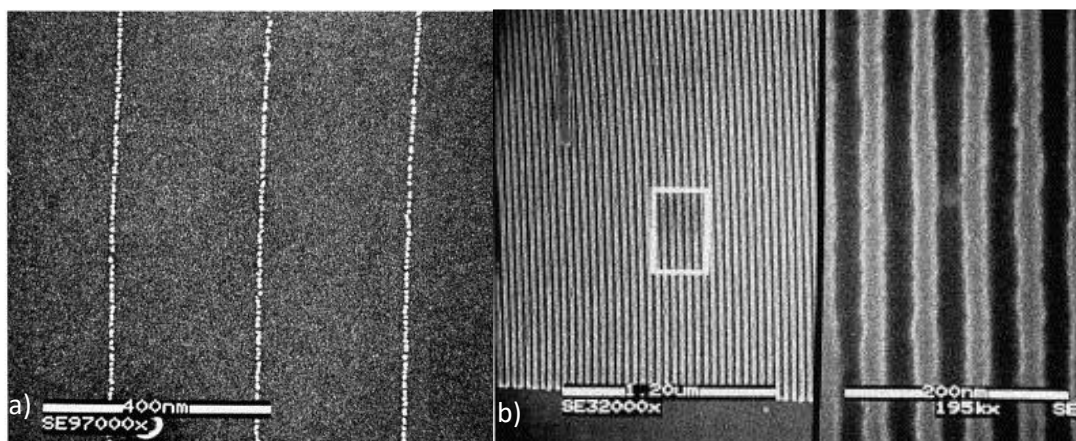


Figure 4.4 SEM image of a) sub-10 nm lines obtained by lift-off of a gold film, b) 20-nm line and space array [51]

Evaluation of negative tone resist, ma-N 2400, was focused on using an electron beam exposure tool [52]. During the experiment, the resolution capability of ma-N 2400 DUV negative tone resist was controlled by exposing the nanometer region. Secondly, extreme aspect ratios of dense patterns were determined. At last, with lower acceleration voltage ( $<20$  V), electron beam exposures were carried out to determine the properties of resist. In resist layers of 800 nm thickness, a high aspect ratio of nearly 5 patterns can be generated. In a thinner resist layer, dense lines and spaces in the sub-100 nm region can be produced. Minimal feature size was 50 nm. For a low voltage EBL, this negative resist has well good sensitivity and high-resolution capabilities for all energies. Fig. 4.5 shows all types of lines at different dose values.

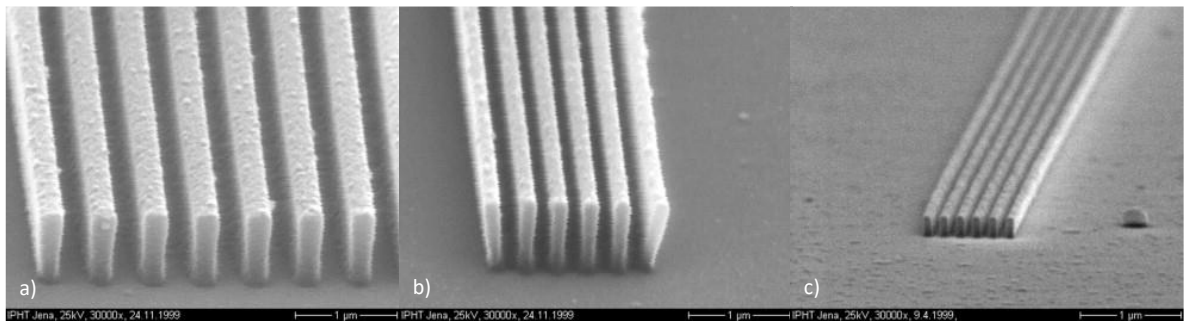


Figure 4.5 SEM images of lines and spaces with the dimension of a) 250 nm with a dose of  $160 \mu\text{C}/\text{cm}^2$  and thickness of resist 800 nm , b) 150 nm with a dose of  $200 \mu\text{C}/\text{cm}^2$  and thickness of resist 800 nm, c) 80 nm with a dose of  $120 \mu\text{C}/\text{cm}^2$  and thickness of resist 180 nm [52]

Elsner, H et al. [52] achieved undercut length up to 300 nm by a LOR/PMMA bilayer resist and dissolved LOR layer in a diluted solution such as CD26, developer for UVIII. As a result, 30 nm trenches were observed with a clear undercut. In the lift-process, successful lift-off for lines of metals with 20 nm in width was fabricated.

3 nm NiCr wires whose pitch among them was arranged as 100 nm were fabricated by 50 nm thick double layer of PMMA with EBL and beam current was set to 12 pA at 100 keV [53]. After exposure and development with MIBK: IPA (1:3), the deposition of 10 nm layer of NiCr and lift-off process were performed. They claim that wires in the unexposed area are produced by secondary electron, not a primary electron. They concluded that if the electron dose is too high, then lines will be continuous.

Lines having a feature of 3-4 nm width and 80 nm pitch were obtained in 40 nm thick PMMA resist by using EBL at 80 keV and spot size less than 4 nm as shown in Fig.4.6 [54]. Together with the use of nonsolvent-based developer systems, water: IPA, fabrication of the narrow linewidth was made possible since that developer system prevents nanostructures from taking long developing time so that swelling of unexposed part can be limited.

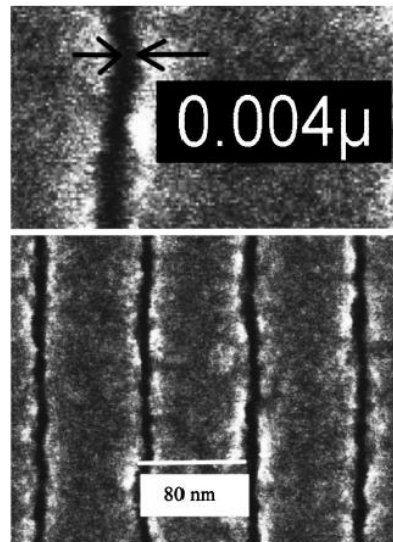


Figure 4.6 SEM image of 80 nm pitch in PMMA with 4 nm linewidth [54]

A study for exposure parameters of e-beam lithography was presented [39]. Beam voltage, apertures diameter and resist thickness were tried to optimize to succeed fabricating smaller dimensions for each resist thicknesses. They reached some results indicating that when beam energy and resist thickness are made larger, less energy deposition has occurred throughout resist and so large amounts of the dose is required to expose smaller dot size. The effective range of forwarding scattering is between 50 and 170 nm, and the backscattering range is nearly 560 nm when the larger dimension is exposed, and thus larger size should be exposed with a lower dose.

Fabrication procedure of a bowtie structure on the insulating layer using the EBL process along with the bilayer resist was presented [12]. Bowtie structure is the next generation for the optical probe. It was expected that having a 40 nm gap in the bowtie structure is behaved as resonant elements to provide spatial resolution. In the fabrication procedure, as a substrate, Pyrex glass was used to be transparent to the incident wave source. PMMA was coated to cover Cr layer preventing insulator substrate from charging problem. Then

after gold evaporation, unwanted materials were removed by lift-off.

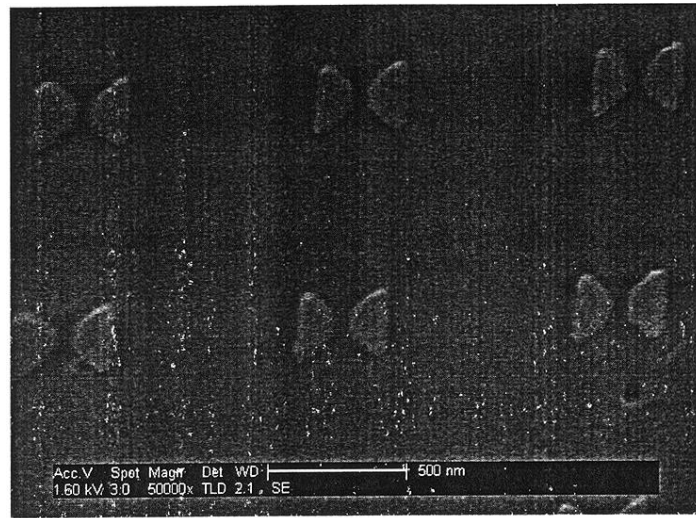


Figure 4.7 SEM image of Nanobowtie structures using bilayer resist [12]

## CHAPTER V

### NANOFABRICATION RESULTS

#### 5.1. Nanofabrication

High technology and facilities are necessary to fabricate extremely small devices from wafer technology. During the thesis, since fabrication of devices is at the nanoscale, electron beam lithography (EBL) is preferred.

This chapter will explain the method which is used in nanofabrication and the flow of the process. The device fabrication is generally performed methods of e-beam lithography, e-beam evaporation and lift-off process in the cleanroom of Sabancı University Nanotechnology Research and Application Center (SUNUM) and field emission scanning electrostatic microscope (FE-SEM) room facility in Faculty of Engineering and Natural Sciences in Sabancı University.

#### 5.2 Wafer Preparation and Cleaning

A 4-inch wafer of glass, silicon and 500 nm  $S_3N_4$  film grown on silicon are used. Each wafer is cut into 2×2 cm squares with wafer scribe or disco wafer dicer. The usual cleaning process is started with substrates placed into glass beaker filled with acetone and then sonication is made into acetone to remove contamination, which might lead to poor adhesion or formation of a defect in the resist. After that, samples are waited in a glass beaker with clean acetone to remove the rest of the residual from sonication. The next

step is to prepare clean isopropanol (IPA) and put the sample into it. When the sample is removed from IPA baker, the last step is to wash the sample with DI water, and it is blown using  $N_2$  gun. Then, samples are baked in the oven at  $135^\circ\text{C}$  for dehydration to make desorption of  $H_2O$ .

### 5.3 Electron Beam Lithography

Electron beam lithography is capable of fabricating submicron structures. For that purpose, there are three steps for the flow of process; exposure of the sensitive material, development of resist and transferring of patterns on the substrate. Each step is connected to each other and should not be considered independently. To fabricate sub-50 nm nanostructures, each step should be optimized and considered carefully to demonstrate their accumulative effect on the rest of the process. In the resist structures, when a beam of the electron is exposed to resist, some changes can be occurred because of the chemical structure of resist. It is called a positive resist when the region which is exposed to electrons becomes solvable. If it is a negative resist, the unexposed region will become soluble.

During the thesis, PMMA, positive resist, primarily is used due to providing high resolution with ease of the process, low cost [36] and availability at different compositions, concentrations and weight. PMMA contains a long polymer chain with masses of 495 and 950K MW [9]. When they get the amount of energy from the electron beam, chemical transformation reaction happens, resulting in breaking polymer backbone bonds and many scission events have occurred. Then, the developer removes resulting fragments selectively. The sensitivity and contrast of PMMA are inversely proportional to their molecular weight due to the lower solubility of higher molecular weight [20]. In terms of resolution, higher molecular weight allows to higher resolution because the higher molecular weight in the lithography process is broken into smaller molecular chain scission less than the lower one [10]. As a result of low sensitivity to electrons in higher molecules, the development rate is slower, and resolution is better than low molecular PMMA. The concentration rate determines the viscosity of PMMA. Concentration and spin-speed have a critical influence on the thickness of resist. PMMA is available for

many kinds of weight forms such as 495 and 950K MW by making a correlation with different casting solvents such as chlorobenzene and anisole with different concentrations. During the coating activity on the wafer, most of the solvent is evaporated and the remaining amount of solvent can be eliminated by baking at a specific temperature which is provided by resist manufacture. After exposure, developer dissolves the only exposed part for positive photo resist. Methyl isobutyl ketone (MIBK) is widely preferred developer for PMMA. However, since development rate of MIBK is very fast, it should be diluted with IPA to get better control and resolution.

In this thesis, the lithography process has been performed with the Vistec EBPG 5000+ES 100 kV Electron beam lithography (EBL) system which provides a very low spot size of  $\approx 2$  nm, low exposure current [55]. A standard operating procedure for the Vistec EBPG500+ EBL system is given in the Appendix. A. The feature list of EBL is given in Table 5.1. Fabrication recipe for the nanostructures is summarised in the following;

Table 5.1 Specific parameters for Vistec EBPG500+ EBL

<b>Parameter</b>	<b>Details</b>
Acceleration Voltage	100 kV
Beam Current	from 50 pA to 300 nA
Spot Size	from $\sim 3$ to 350 nm (defocussed)
Main Field Resolution	from 1.25 to 7.812 nm
Main Field Size	from 81.92 to 512 $\mu\text{m}$ (16 bit)
Beam Step Frequency	from 500 Hz to 25 MHz
Alignment	< 20 nm
Subfield Resolution	from 0.0781 to 0.488 nm
Subfields Size	from 1.28 to 4.525 $\mu\text{m}$ (14 bits, 100 kV)
Beam Step Size	from 0.0781 to 125 nm

**Step 1:** Wafer is spin-coated with a layer of 495 Polymethyl-methacrylate (PMMA) C4 resist at 4000 rpm for 45 seconds, then 270 nm resist layer is grown.

**Step 2:** Wafer is baked on a hot plate at 180°C for 10 minutes to remove the excess solvent

**Step 3:** Wafer is spin-coated with a layer of 950 Polymethyl-methacrylate (PMMA) C2 resist at 3000 rpm for 45 seconds, then 100 nm resist layer is grown as seen Fig.5.1b.

**Step 5:** Wafer is baked on a hot plate at 180°C for 10 minutes to remove the excess solvent and eliminate shear stress caused by spin coating.

**Step 6:** Electron beam lithography (EBL) is performed to expose bilayer PMMA structures with different dose values, which are 550, 700 and 800  $\mu\text{C cm}^{-2}$  at 100kV. Proximity effects for the fabrication are taken into consideration by performing an automated proximity effect correction algorithm.

**Step 7:** Mixture of Methy isobutyl ketone (MIBK) and isopropyl alcohol (IPA) is used to develop and dry in  $N_2$  flow as illustrated in Fig. 5.1c.

**Step 8:** To remove the thin layer of PMMA in the structures, oxygen plasma is performed for 10 seconds.

**Step 9:** To evaporate metal, the wafer is placed in evaporator machined named as TORR Instruments with e-beam evaporation, then, chromium and gold metals Cr/Au (4/50 nm) are deposited after reaching the vacuum level under  $\approx 6 \times 10^{-6}$  mBar as demonstrated in Fig. 5.1d.

**Step 10:** To lift the metal off, the wafer is immersed into acetone and left for a specific time to let acetone make diffusion underneath PMMA. Based on the final structure of PMMA, if lift-off is not achieved, ultrasonic vibration can be helpful as shown in Fig. 5.1e.

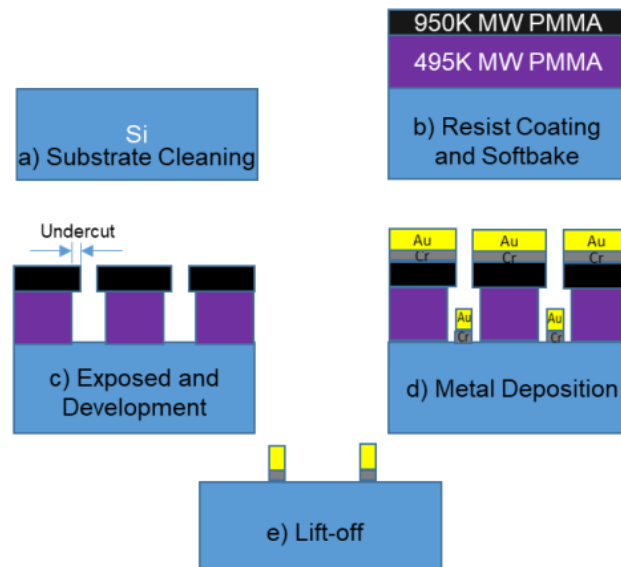


Figure 5.1 Summary of nanofabrication process flow

Before looking at parameters of nanofabrication, each lithographic process has an optimum dose range to the pattern desired nanostructures with as possible as less change in their dimensions. Some exposure performances referred to dose tests usually are required. In this dose test, the same patterns are exposed at different doses on the same substrate (e.g. Si, glass or silicon nitride coated on silicon). In our work, to determine related dose values, which will be used to expose samples during optimization steps, dose range that is from 400 to 950,  $\mu\text{C cm}^{-2}$  was performed in the silicon substrate by applying the fabrication steps mentioned in Fig.5.1. After a fixed development process was applied, optimum dose values, which are 550, 700 and 800  $\mu\text{C cm}^{-2}$  were determined through examination in detail by optical microscopy in seen in Fig.5.2. Smaller than 550  $\mu\text{C cm}^{-2}$  was not performed a process of lift-off very well and also sensitivity range for PMMA of 495 and 950K MW is 800  $\mu\text{C cm}^{-2}$  [24,36]. To optimize the fabrication process of nanostructures by EBL and become a suitable candidate for the fabrication of nanostructures, some important parameters will be discussed.

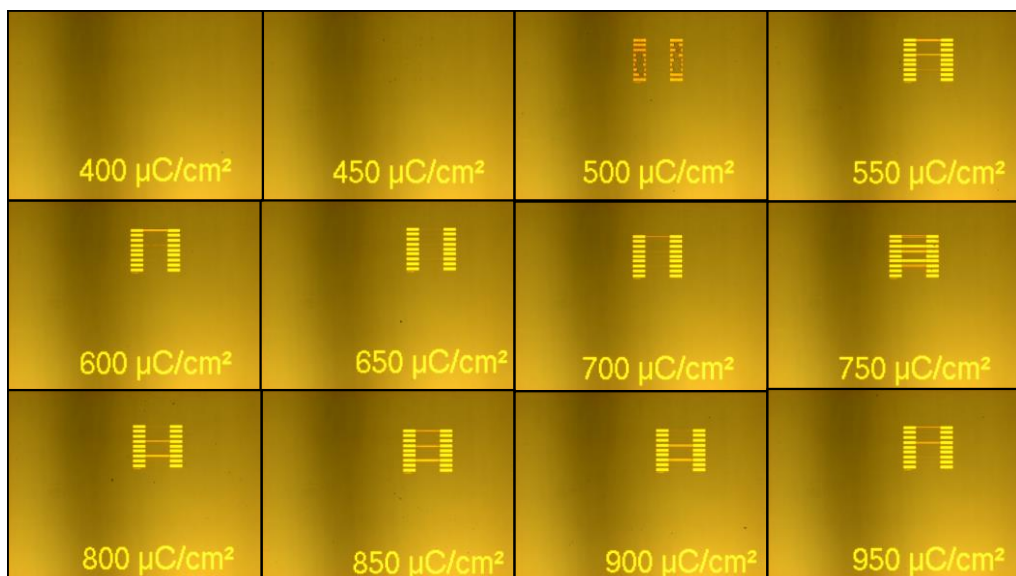


Figure 5.2 Optical images of the dose spectrum

## 5.4 Discussion of Parameters

### 5.4.1 Exposure Dose

The first parameter is to control the optimum value of e-beam dose which is the amount of energy applied to per unit area. For each type of lithographic process, the optimum dose is available to represent the dose at which the value of measured linewidth is nearly close to actual linewidth with a minor change in critical dimension (CD). Since acceleration voltage and aperture size are fixed during the exposure, beam current is not changed [49]. Then, exposure dose is measured with respect to current exposed to per unit area  $\mu\text{C cm}^{-2}$ . Dosage which is required to break connection structure of the electron resist determines the size of the exposed pattern [49]. Obtaining results from specific dose values should be analyzed in detail to decide related parameters to reach the desired nanostructures. When beam overexposes resist structure which means that resist receives more amount of beam of electrons than its threshold value, PMMA in interwires is partially exposed more since Gaussian intensity profile is created by both forward and backward scatterings and energy distribution of overall dose is the sum of all individual Gaussian distribution as seen Fig. 5.3a [46,27]. As supposing the same development time, when the e-beam dose is increased, the dose profile in the gap region increases and narrower interwires gaps are expected.

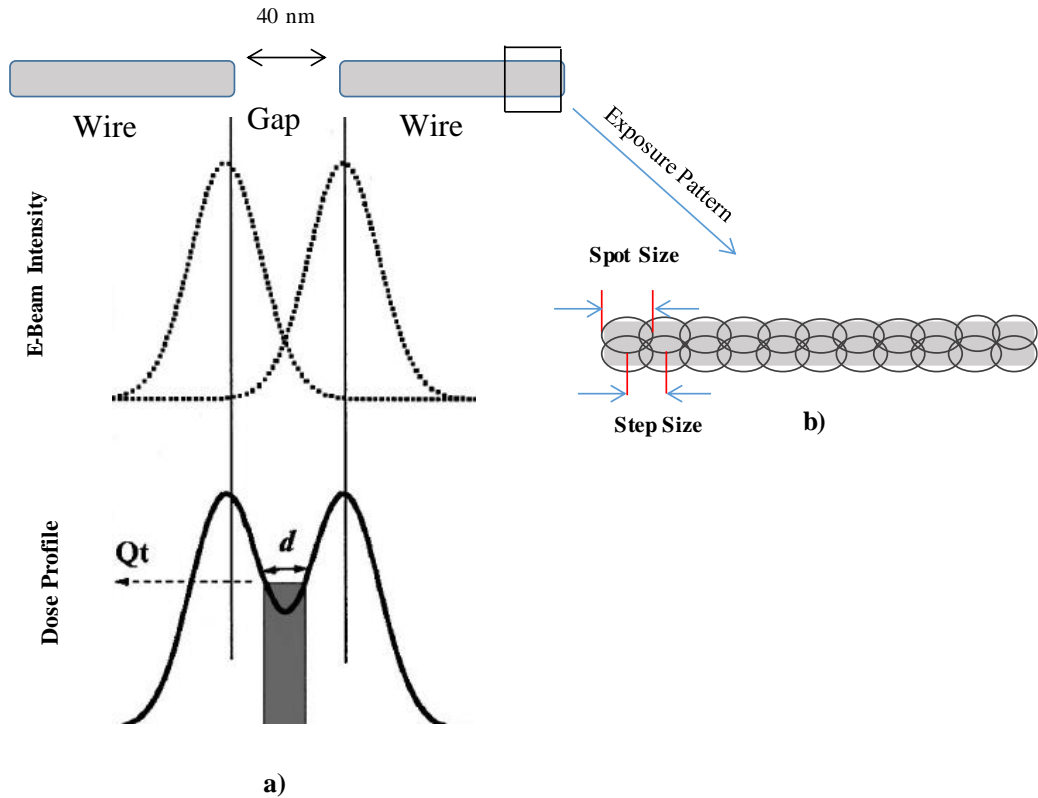


Figure 5.3 Schematic explanation of fabrication mechanism

When PMMA which is in the gap region has been exposed than optimal value, it has been developed more and the remaining undeveloped part determines the actual resulting size for the actual interwire gap. As the dose is increased, the amount of energy deposited in the resist is increased and a large amount of resist reaches the threshold energy to become developable. Exposure is performed by scanning the beam once over single exel (one line) called a single pass over one line. Our writing strategy is based on the vector scanning which the beam is deflected only over the entities to be exposed. To produce the thinnest structure, exposure contains filling of the areas by a finite number of the scan of the electron beam as illustrated in Fig.5.3b. To minimize the proximity effect, the step size determined by beam current must be equal to half of the spot size [27].

A set of the test was performed with different exposure values,  $550 \mu\text{C cm}^{-2}$ ,  $700 \mu\text{C cm}^{-2}$  and  $800 \mu\text{C cm}^{-2}$  which were determined from the dose test, under the same fabrication parameters such as; developer type and developing time, bake time and temperature to obtain specific dimension for nanostructures. Same development conditions were performed by immersing in MIBK: IPA (1:3) and MIBK: IPA (1:1) respectively and drying with  $N_2$ . Fig. 5.4 shows scanning electrical micrographs (SEM) image of the gap regions produced under the different exposure doses. When the same

predesigned 40 nm and 50 nm gaps were written at  $550 \mu\text{C cm}^{-2}$ ,  $700 \mu\text{C cm}^{-2}$  and  $800 \mu\text{C cm}^{-2}$  sequentially, gap width was broadened since more electrons were transferred to PMMA resist and sizes of gap region became narrower for the substrate of silicon with a 500 nm thick layer of PECVD nitride.

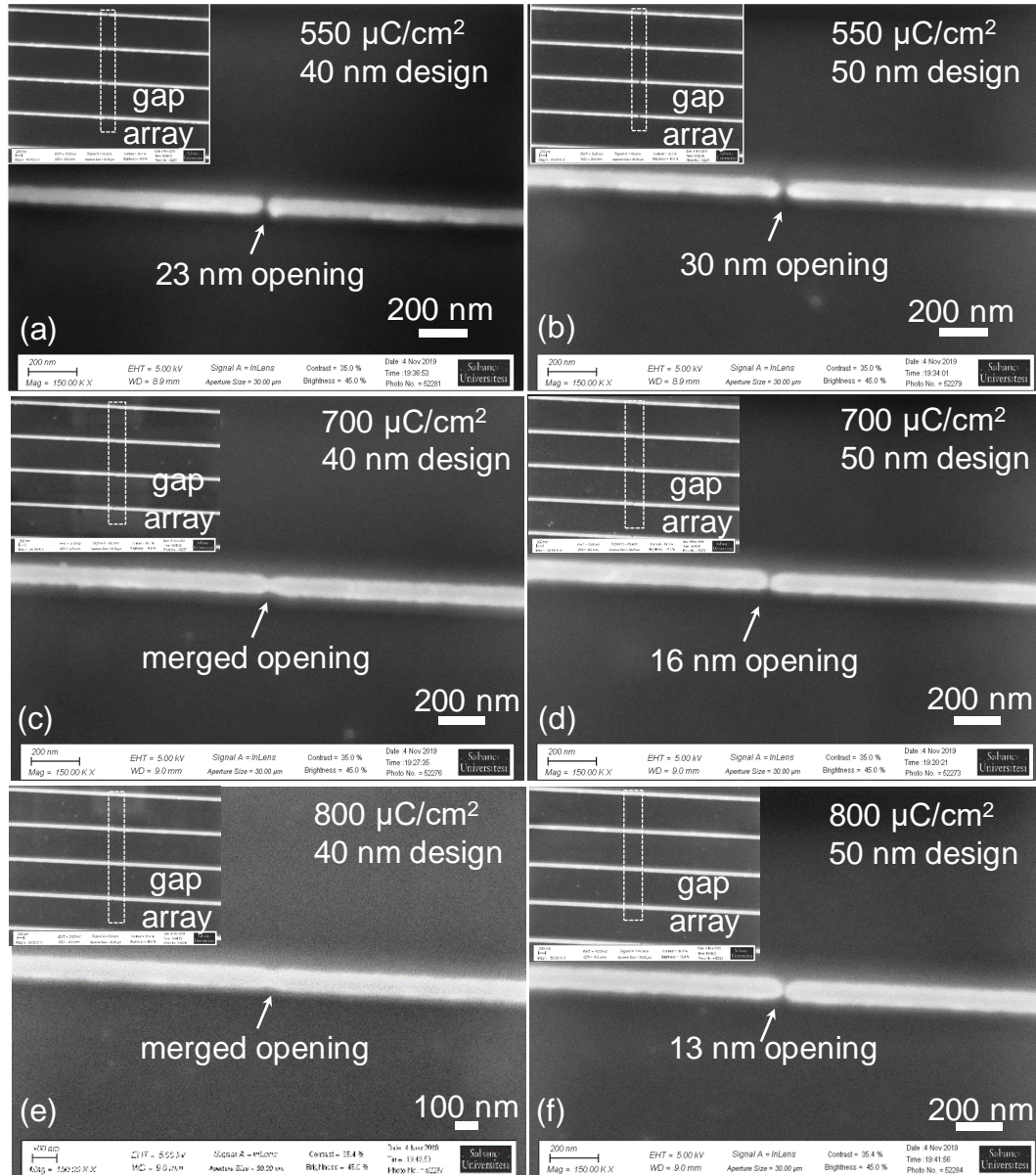


Figure 5.4 SEM images of the gap nanostructures fabricated with the same development time for predesigned 40 and 50 nm gaps with various exposed dose values respectively; a) and b)  $550 \mu\text{C cm}^{-2}$ , c) and d)  $700 \mu\text{C cm}^{-2}$ , e) and f)  $800 \mu\text{C cm}^{-2}$  for substrate of silicon with a 500 nm thick layer of PECVD nitride

The same conditions also were repeated for silicon substrate as illustrated in Fig.5.5. By keeping the same development conditions, MIBK: IPA (1:3) and MIBK: IPA (1:1), respectively, but increasing the e-beam dose to  $550 \mu\text{C cm}^{-2}$ ,  $700 \mu\text{C cm}^{-2}$  and  $800 \mu\text{C cm}^{-2}$

$cm^{-2}$  sequentially, the gap was also getting closed for silicon substrate respectively. In Fig. 5.5a and 5b, development time for nanopatterns written with  $550 \mu C cm^{-2}$  was not enough to clean PMMA in the exposed region and so, during lift-off a piece of structures were broken.

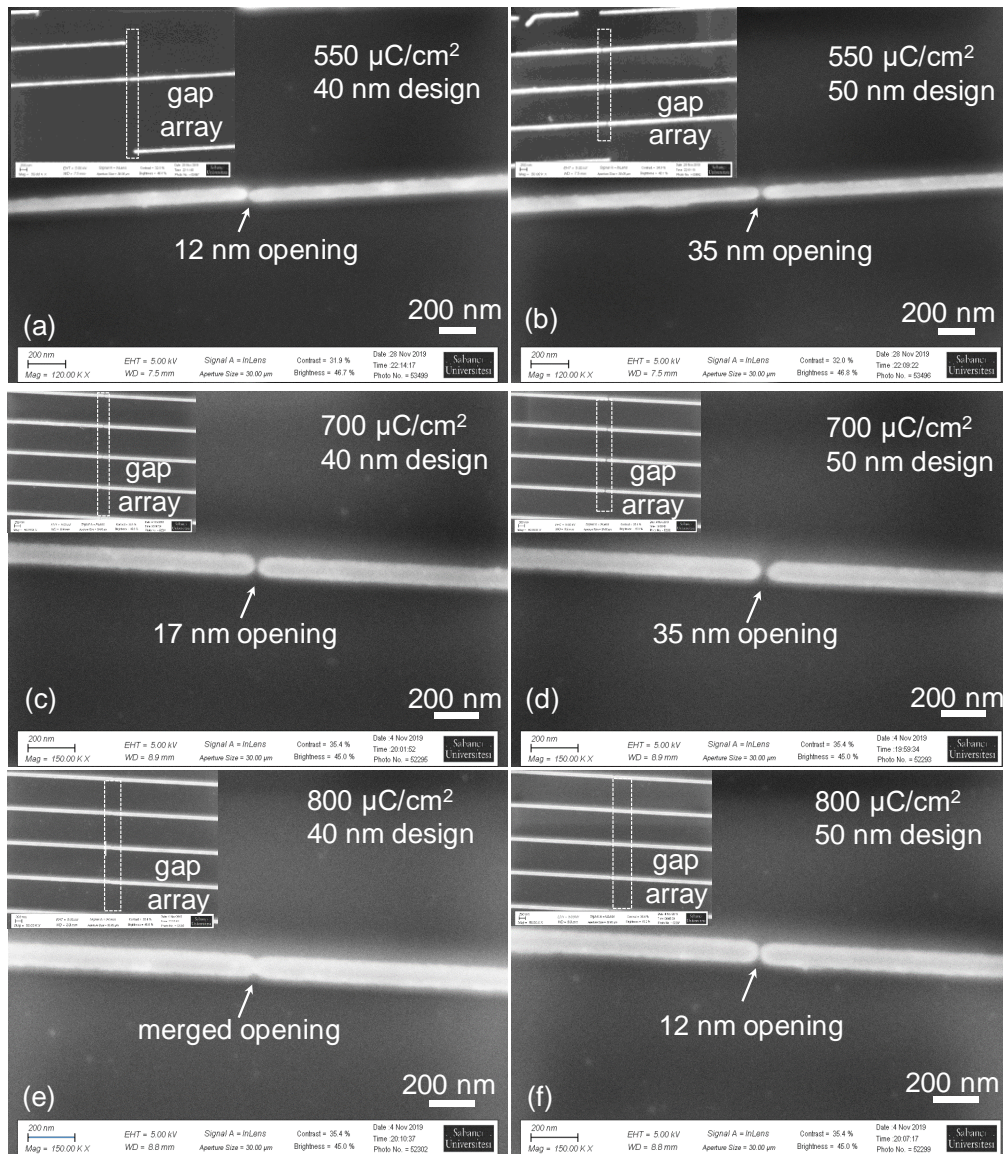


Figure 5.5 SEM images of the gap nanostructures fabricated the same developing time and type for pre-designed 40 nm and 50 gaps with various exposed dose values respectively; a) and b)  $550 \mu C cm^{-2}$ , c) and d)  $700 \mu C cm^{-2}$ , e) and f)  $800 \mu C cm^{-2}$  for substrate of silicon

If a lower dose compared to the optimum dose is exposed to the pattern, the width of the actual structure is narrower than the width of the designed structure. On the opposite side, overexposure in which dose is higher than the optimum dose widens the pattern size [9]. By keeping the same design, 50nm, for every exposure with a different value of exposure

doses,  $550 \mu\text{C cm}^{-2}$ ,  $700 \mu\text{C cm}^{-2}$  and  $800 \mu\text{C cm}^{-2}$  sequentially, the related results were shown in Fig.5.6. Samples were immersed in MIBK: IPA (1:3) and MIBK: IPA (1:1) respectively and drying with  $N_2$ . When the dose was increased, the amount of energy deposited in resist was increased and threshold energy becoming developable was achieved in the great percentage of resist. By increasing the dose, the line width was increased since for higher doses, a great amount of electron was transferred to resist more efficiently.

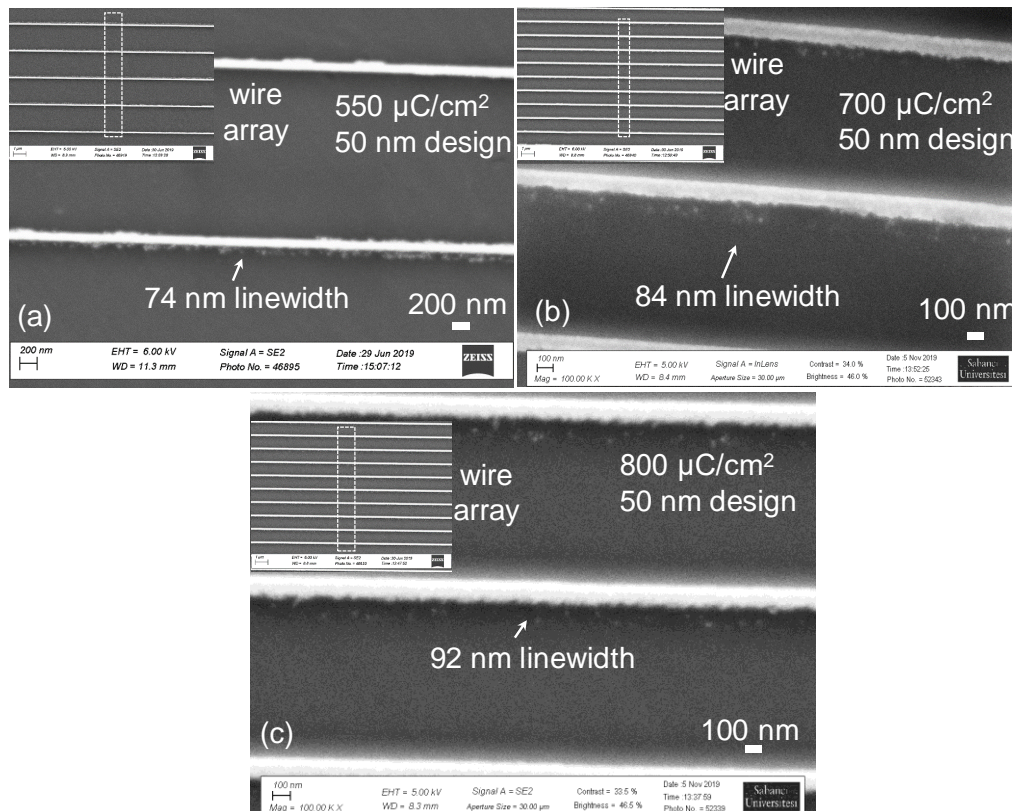


Figure 5.6 SEM images of the fabricated wires nanostructures with the same development time and type, but different doses of a)  $550 \mu\text{C cm}^{-2}$  b)  $700 \mu\text{C cm}^{-2}$  c)  $800 \mu\text{C cm}^{-2}$  for substrate of glass

#### 5.4.2 Development Time

The development process plays a critical role in acquiring nanostructures as a result of e-beam patterning together with exposure dose. Theoretically, it is difficult to make a prediction and only experimentally is determined to which kinds of developer types and how much of time for development is applied. Development can be described as immersion samples into solution, which is formed by a real solvent of the resist and a

resist-non solvent part, for a certain time. After exposure, liquid developer dissolves the fragments or non-crosslinked molecules. During the development, the solvent spreads into the polymer matrix and starts to surround the fragment. While molecules begin to interact, a gel is started to form [9]. The amount of fragmentation and strength of the solvent are two factors to determine the thickness of the gel layer [10]. As surrounded by solvent, the fragments are separated from the matrix and diffuse into the solvent. Generally, longer fragments are not able to move quickly and take longer time due to the relation of the amount of dose exposed and average fragment size means that as dose increases, fragment size decreases and solubility of developer increases [10]. The critical part of development is to determine the ratio of composition into developer mixture and development time. Methyl isobutyl ketone (MIBK) is a developer of PMMA and its developer rate is controlled by mixed with non-solvent. MIBK mixed with isopropanol (IPA) in ratio 1:3 has low sensitivity, but high contrast, whereas a 1:1 ratio improves sensitivity as changing contrast less [20]. In general, the effect of development time on the resolution does not seem to be significant, especially large structures written in thick resist [9]. However, development time may become important when nanostructures are patterned on a thin layer. In case of longer development for the sample, the structures are either washed away or etched.

In the first case, pattern developing time was arranged to 210 s by MIBK mixed with IPA in ratio 1:3 as shown in Fig.5.7a, and 7b and then increased to 300 s in illustrated in Fig.5.7c and 7d without changing exposure dose,  $550 \mu\text{C cm}^{-2}$ , and develop type, MIBK: IPA (1:3). The interwire gap was getting narrower and narrower when development time was increased. In the second case, increasing developing time, especially for a high dose of  $800 \mu\text{C cm}^{-2}$ , caused etched away in the sidewall of wires as seen in Fig.5.7e. The reason is that additional dose enables to create more amount of short fragment size and hence development time should have been arranged less than 300 s to make compensation between the time of development and exposure. Resist swelling might occur for long development. Patter distortion and additional stress may be induced at the cost of loss shape deformations.

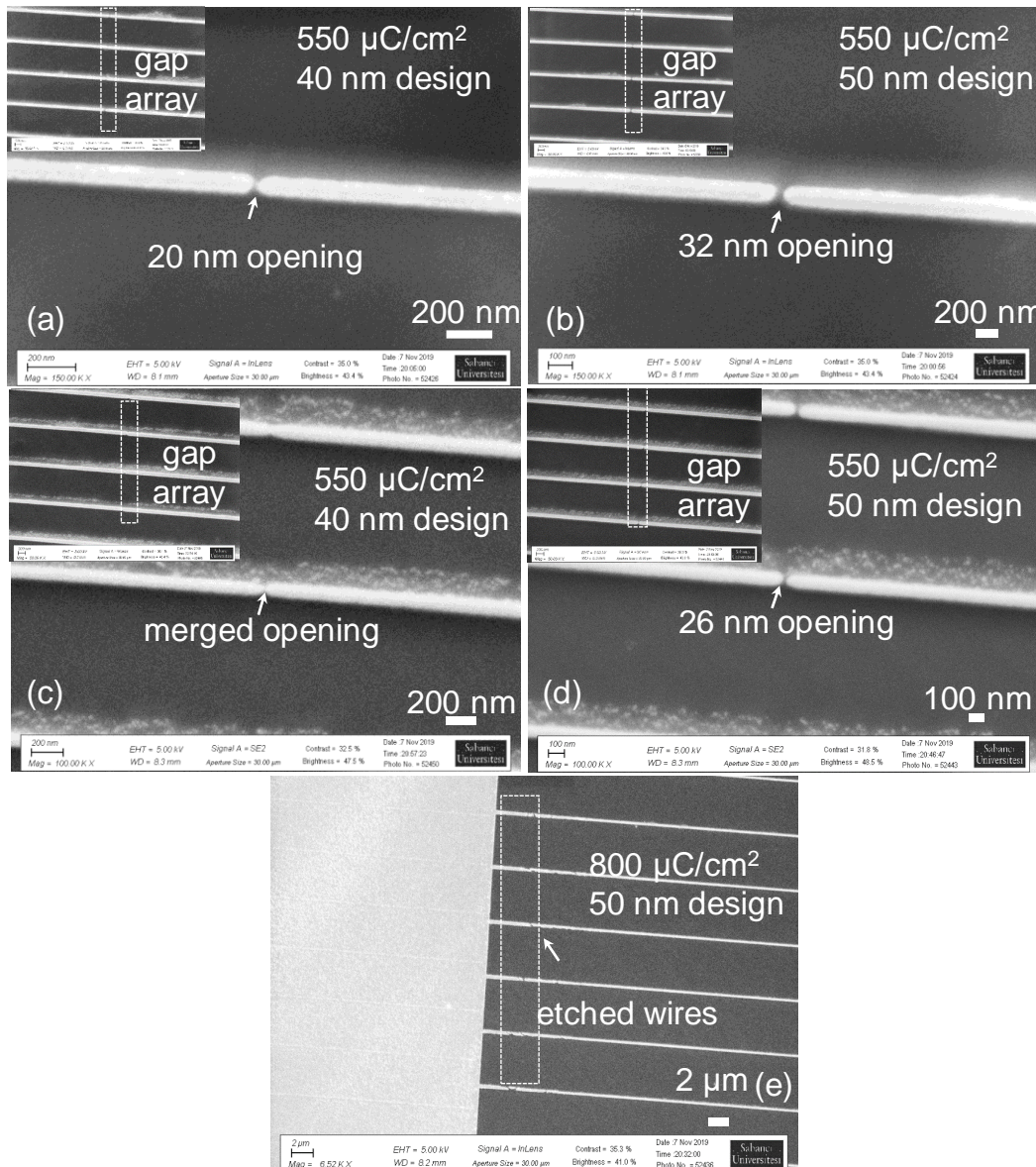


Figure 5.7 SEM images of the fabricated predesign 40 nm and 50 nm gap nanostructures with the same exposure dose  $550 \mu\text{C cm}^{-2}$  and development type (MIBK: IPA (1:3)), but different development time respectively; a) and b) 210s, c) and d) 300 s, e) etched sidewall of wire exposed with  $800 \mu\text{C cm}^{-2}$  in glass substrate with 300 s.

To observe the development time effect on employing MIBK mixed with IPA in 1:3 and 1:1 together, this study was performed by measuring the linewidth of nanostructures. Resist swelling might be occurring for developers, especially for long-time development [31]. Fig.5.8 below shows the effect of increasing developing time for wire structures by corresponding development time of MIBK mixed with IPA in 1:3 and 1:1 without changing exposure dose,  $800 \mu\text{C cm}^{-2}$ , respectively. It was shown that as developing time is increased; the width of wire structures is also increased. In general, in Fig 5.8a,

the ultimate resolution for the given condition is reached in terms of length of the gap and line width to some extent. However, without considering that conditions, when you increase development time more, the linewidth is broadened as if wires behave as increased in the exposure dose. It should be noted that exposure dose and development time are interrelated to each other as short exposure and long development can be equal to heavier development and short development.

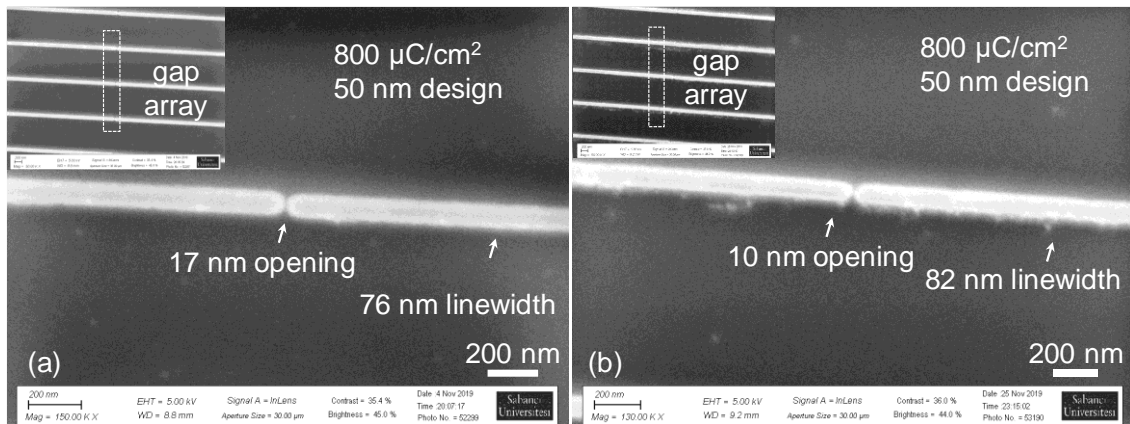


Figure 5.8 SEM images of the fabricated gap nanostructures with the same exposure dose,  $800 \mu\text{C cm}^{-2}$  and, MIBK: IPA (1:3) and (1:1), but different development time respectively; a) 60 s and 5 s, b) 100 s and 5 s in the substrate of silicon

### 5.4.3 Developer Concentration

Along with development time, developer concentration is also other parameters in improvement on the resolution. Making critical observations for each developer concentration is necessary to reach sub-50 nm for nanostructures. MIBK is a strong solvent for PMMA and to dilute it, water or IPA referred to as “nonsolvent” are used. When a low developer concentration is used, the sensitivity increases, structures whose dimensions are under micrometer can be obtained by observing less change in gap and linewidth. Table 5.2 shows the relation between contrast and sensitivity [41]. Observing the effect of developer condition on the nanostructures was performed.

Table 5.2 List of commonly used composition and effect on resolution and sensitivity [41]

<b>Composition</b>	<b>Resolution</b>	<b>Sensitivity /Throughput</b>
MIBK:IPA (1:1)	High	High
MIBK:IPA (1:2)	Higher	Medium
MIBK: IPA (1:3)	Very High	Low
MIBK	Low	High

Fig. 5.9a and 9b represented nanostructures developed with MIBK was diluted by IPA in a ratio of MIBK: IPA (1:3) to acquire accurate features. It was seen that gap structures exposed to  $800 \mu\text{C cm}^{-2}$  were opened largely. The next step was to review development concentration for the same structures. MIBK: IPA (1:1) was included in the fabrication process together with MIBK: IPA (1:3) to see the effect of the higher developer on the gap structures. Since MIBK: IPA (1:1) is a stronger developer; samples were immersed in it for a few seconds. For that time, patterns were exposed to the same dosage and lift-off was actualized successfully as illustrated in Fig 5.9c and 9d. Comparing to Fig.5.9a and 9b, it was seen that since the stronger developer, MIBK: IPA (1:1), was used together with MIBK: IPA (1:3), length of the gap of structures was reduced significantly. The addition of high concentration for process development leads to increase sensitivity but to reduce resolution compared to only performing the development process with MIBK: IPA (1:3). The potential risk of using strong developer as writing nanostructures is that structures exposed to higher dosage is likely to be washed away and only highly exposed areas can remain on the substrate.

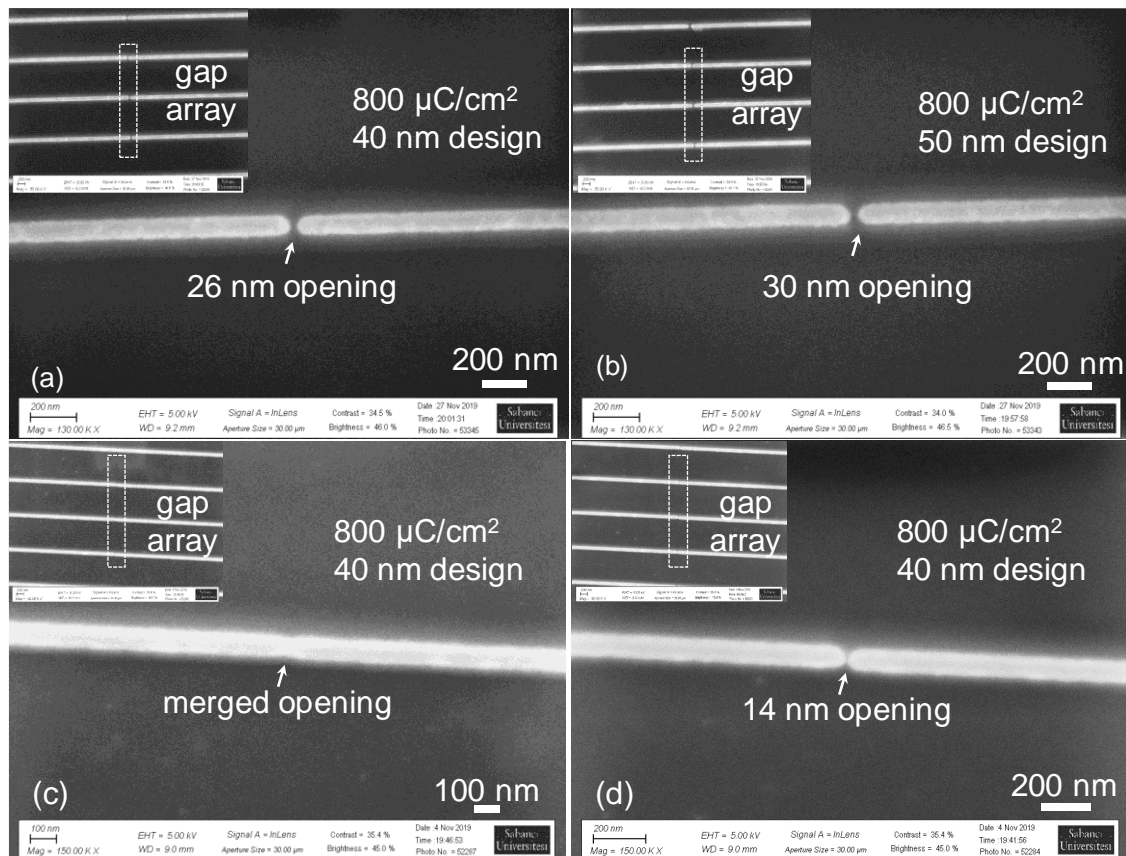


Figure 5.9 SEM images of the fabricated predesign 40 and 50 nm gap nanostructures with the same exposure dose,  $800 \mu\text{C cm}^{-2}$  and same development time sequentially, but different development types of a) and b) only (MIBK: IPA (1:3) ), c) and d) (MIBK: IPA (1:3) and MIBK: IPA (1:1)) in the substrate of silicon with a 500 nm thick layer of PECVD nitride.

#### 5.4.4 Bake Temperature

For the same exposure dose value, the low baking temperature affects exposed line width which is getting larger than high baking temperature [49]. This is because the low linking of the polymer chain is created. Additionally, when the amount of solvent remains at the resist, it is also a negative effect on the contrast and adhesion to substrate by relieving film stresses generated by spin coating. The exposed patterns have low contrast at low baking temperatures. Figure 5.10 shows the features of nanostructures that were baked at 160°C and 180°C. All patterns were written and developed with  $550 \mu\text{C cm}^{-2}$  and (MIBK: IPA (1:3)), respectively. The result proved that since PMMA in gap region has low linking of polymer, after exposure, more amount of PMMA had been developed compared to the nanostructure baked at 180°C. Therefore, the length of the gap region is increased as the baked temperature is increased.

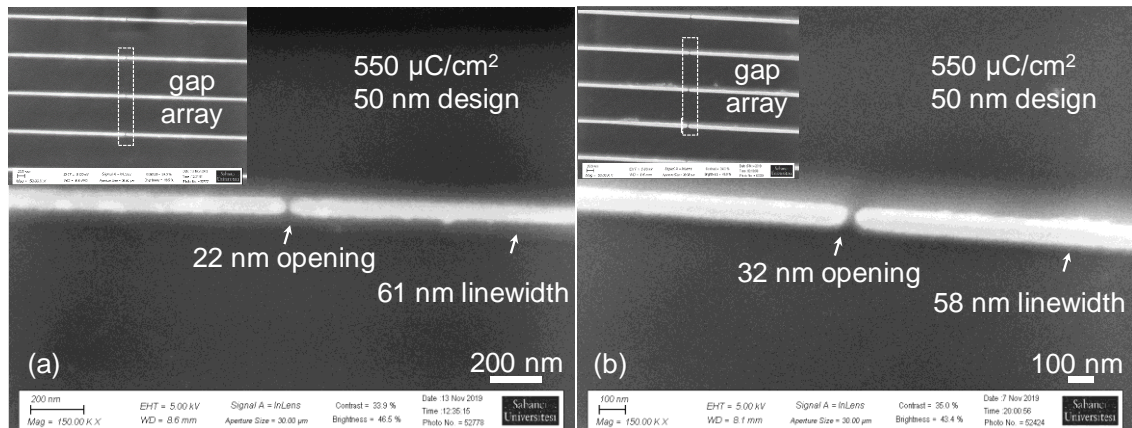


Figure 5.10 SEM images of the fabricated gap nanostructures with the same exposure dose ( $550 \mu\text{C cm}^{-2}$ ), development type (MIBK: IPA (1:3)) and development time, but different bake temperature, respectively; a)  $160^\circ\text{C}$  b)  $180^\circ\text{C}$  in the substrate of glass

#### 5.4.5 Substrate Effect

Analysing the substrate contribution to nanostructures demonstrates the effect on e-beam processes due to their backscattering effect. Three types of substrates; glass, silicon, and silicon with a 500 nm thick layer of PECVD nitride, have been performed to observe their effect on the dimension of nanostructures. To eliminate charge deposition, the conductive layer is coated either on top or underneath of the resist. For the glass substrate, the conducting layer is adopted as a dissipation layer on the top of the resist. Since the lift-off step is required through the fabrication of the features, the Cr layer is spun on top of the resist. The conducting layer helps to transfer more amount of charge to the ground and then as a result, charging is minimized or completely removed [20]. However, in the metal layers, such a metal coating leads to electron beam scattering and hence, causes subsequent broadening of exposure profile at the cost of resolution at the nanoscale [10]. Resist heating might lead to the distortion of the pattern. At 20 keV on Si, about % 20 of the beam power is dissipated as forward or backscattered electrons in resist, whereas the rest is dissipated as heat in the substrate [56]. There is also a relation between substrate and energy absorption. According to theory, with the increase in atomic number  $Z$  of the substrate, elastic scattering increases approximately  $Z^2$  [57]. For that reason, backscattering electron (BSE) is returned from the substrate to resist and re-exposure resist. Fig.5.11 demonstrates results of different substrates without variation in exposure dose,  $700 \mu\text{C cm}^{-2}$ , develop time and type, bake temperature. At the end of the process,

linewidth of nanostructures in Fig.5.11b which all structures were patterned on the glass substrate was broader than silicon substrate.

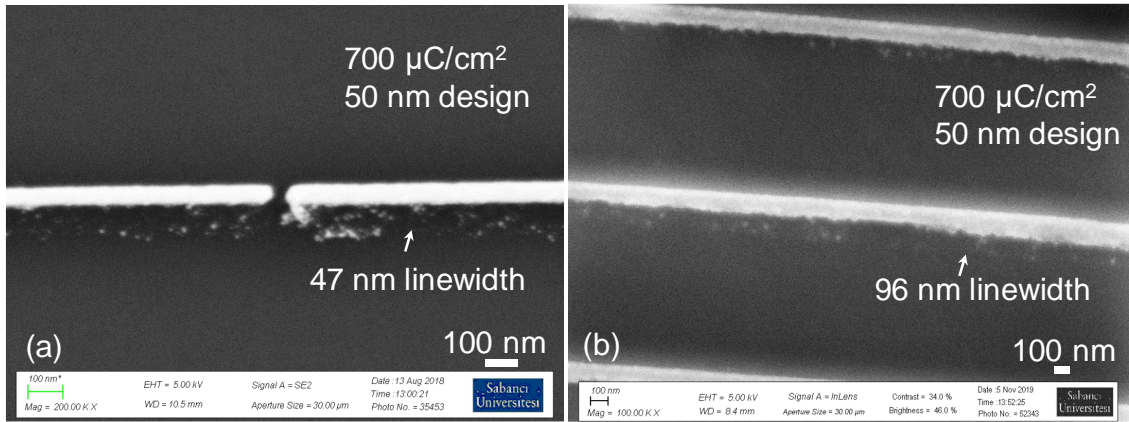


Figure 5.11 SEM images of substrate type on linewidth when the exposure dose ( $700 \mu\text{C cm}^{-2}$ ), developer type (MIBK:IPA (1:3)) and (MIBK:IPA (1:1)) and develop time are kept constant for a) silicon and b) glass substrate.

In the second study, to show the relationship between substrate and energy absorption, two types of the substrate, which are silicon and silicon with a 500 nm thick layer of PECVD nitride, were performed to make a comparison for results. Theoretically, the substrate having a higher atomic number creates more elastic scattering, and so more backscatter electrons are directed to the resist from the substrate, resulting in re-exposure. A thin film, low atomic number  $\text{Si}_3\text{N}_4$ , was grown on bare silicon and made the comparison with silicon wafer. With the same exposure dose,  $550 \mu\text{C cm}^{-2}$ , develop type and time, as illustrated in Fig. 5.12, the linewidth of structures fabricated on  $\text{Si}_3\text{N}_4$  substrate grown on bare silicon is closer to the width of predesigned. Changing the linewidth and length gap structure is less for  $\text{Si}_3\text{N}_4$  substrate grown on Si substrate since in the presence of oxygen atoms which is smaller than silicon atoms in terms of atomic number, numbers of the backscattered electron (BSE) are decreased [58].

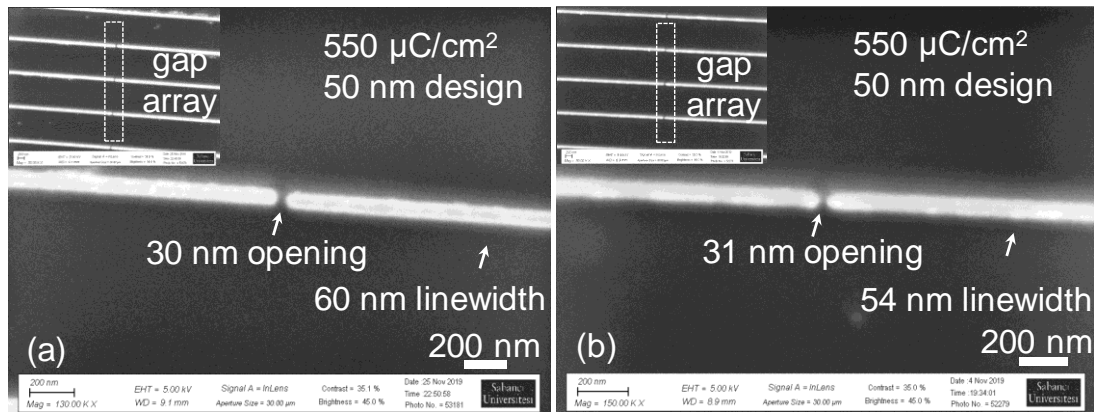


Figure 5.12 SEM images of substrate type on linewidth when the exposure dose ( $550 \mu\text{C cm}^{-2}$ ), develop type (MIBK:IPA (1:3) and MIBK: IPA (1:1)) and time is kept constant for a) silicon and b)  $\text{Si}_3\text{N}_4$  on bare silicon

#### 5.4.6 PEC Effect

The proximity effect in EBL is key requirements with accurate correction for the fabrication of nanoelectronic. VISTEC EBPG 5000 has a limited number of dose classes. To overcome the hardware limitations, software called Layout BEAMER<sup>3</sup> is used. With this technique, artificial dose classes are more than the existing number of dose classes in the machine. Monte Carlo simulation has derived the point of spread function (PSF) used for PEC calculation [45]. The benefit of PEC is not the only development in dimension and also improvement in line edge roughness [45]. To evaluate the potential benefit of PEC, designs are classified into; no PEC and standard PEC, which is selected by prepared PEC files, based on the type of substrate, amount of resist thickness and acceleration voltage of EBL machine. Fig 5.13a and 13b show structures in which PEC was not included in fabrication process. Dosage was selected as  $550 \mu\text{C cm}^{-2}$  on silicon substrate and develop type was MIBK: IPA (1:3) and MIBK: IPA (1:1). After lift-off process, it is seen that all of lines were broken. In the next step, by keeping the all parameter as a same, but prepared PEC was included in EBL machine so that required dose range can be classified based on distance of wire to each other. Figure 5.13c and 13d represents the nanostructures including PEC package in wire region. Without changing previous experimental conditions, process was performed, and it was seen that proper fabrication

<sup>3</sup> <https://genisys-gmbh.com/beamer.html>

was acquired and gap regions were opened. By the proximity correction, different dose for each pixel or location in nanostructures is applied for each individual shape.

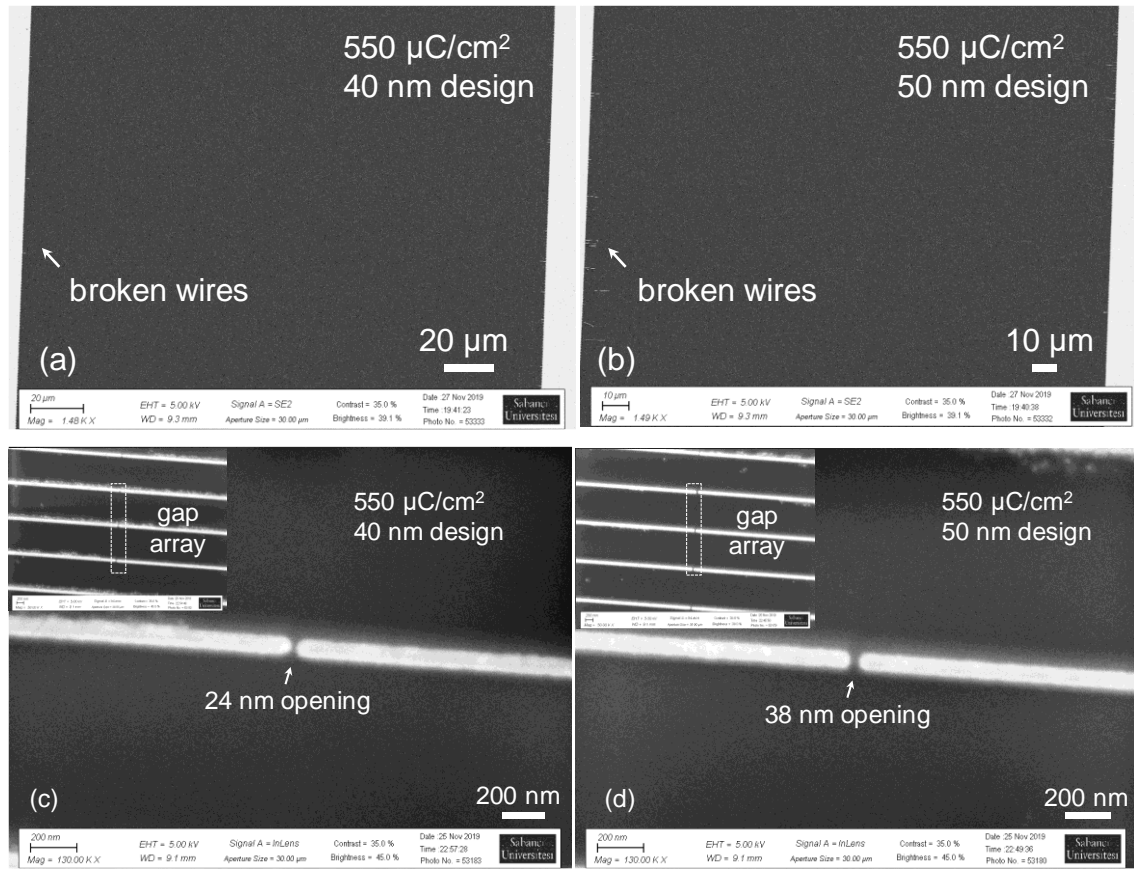


Figure 5.13 SEM images of PEC on gap nanostructures when the exposure dose ( $550 \mu\text{C cm}^{-2}$ ), developer type (MIBK:IPA (1:3)) and (MIBK:IPA (1:1)) and develop time are kept constant for a) and b) no PEC , c) and d) PEC for silicon substrate.

In the second case, wire nanostructures were tried to fabricate with a dose of  $800 \mu\text{C cm}^{-2}$ , type of development of the only MIBK: IPA (1:3) and no PEC. As seen in Fig 5.14a, 14b and 14c, although development time was increased from 130s to 210s to completely remove the exposed polymer molecule for features patterned with  $800 \mu\text{C cm}^{-2}$ , it was not possible to fabricate designed nanowire and also was realized that as development time is increased, the sidewall of wire is broken more. It was proved that clearance of depth of exposed lines is insufficient to generate wire patterns or some part of lines, especially the corner side, should be exposed more compared to the middle part of lines because of being subjected to many scattering effects. That result is manifested by low contrast. However, when PEC for silicon at 100kV was included for the writing stage in EBL machine, dose classification was been able to make and base dose value for

corner region was multiplied by a specific value. Considering the fact, Fig 5.15a and 15b proved that structures including PEC package were fabricated very well without changing any experimental parameters as mentioned in the previous one. Especially, wires broken at the edge of the pattern receive more amount of dose by proximity correction and thus dissolution rate of sidewall areas of wires is accelerated. Differences between the dissolution rate across the wire placed on the different region are reduced [59].

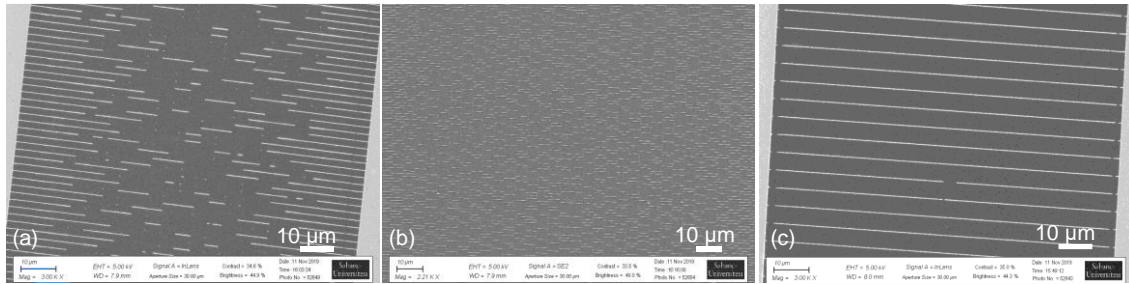


Figure 5.14 SEM images of the fabricated predesign wire nanostructures with the same development type (MIBK: IPA (1:3)), no PEC, exposure dose  $800 \mu\text{C cm}^{-2}$  but different development time, respectively; a) 130 s, b) 180 s, c) 210 s, substrate of silicon with a 500 nm thick layer of PECVD nitride

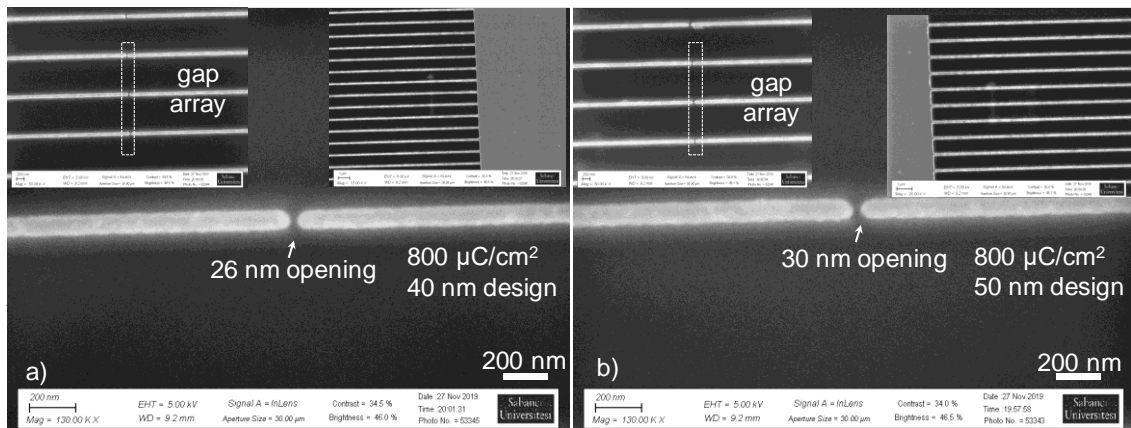


Figure 5.15 SEM images of the fabricated predesign 40 and 50 nm gap nanostructures with the same development type (MIBK: IPA (1:3)), PEC, exposure dose  $800 \mu\text{C cm}^{-2}$ , development time 180s in the substrate of silicon with a 500 nm thick layer of PECVD nitride

## CHAPTER VI

### CONCLUSIONS

In this work, EBL having many interacting parameters affecting the quality of resulting nanostructures and durability of the process was investigated together with performing low cost of PMMA/PMMA bilayer as positive tone resist to create undercut profile and lift-off process by characterizing all results with field emission scanning electron microscopy (FE-SEM). To successfully write nanostructures, one should keep in mind the various factors such as exposure dose, development time and developer type, bake temperature, substrate effect and proximity effect correction (PEC) that limit resolution, sensitivity. Even though some parameters are optimized, it is difficult to obtain structures with sizes equal to the length of predesigned structures.

Selecting a proper value of dosage is one of the significant parameters. When exposure dose is applied more than the threshold value, more electrons are transferred to exposed regions where they become developable. Then, the linewidth of structures is widened. In the case of the amount of gap in nanostructures, PMMA located in the interwire determines whether the desired amount of length for the gap is obtained. When the e-beam exposes the resist more at the tip of each wire, PMMA in the interwire is partially exposed and the interwire gap becomes increasingly narrower. When the e-beam dose is increased, the dose profile in the gap region increases and narrower interwire gaps are expected. In terms of linewidth for wires, as the dose is increased, the linewidth is also increased since, for higher doses, a great amount of electron transfers more efficiently to resist.

Development time and developer concentration also play a critical role in reaching suitable nanostructures. As if development time is seen as less important in the fabrication process, it has also a huge effect on, especially smaller structures. The interwire gap is getting narrower, but the linewidth of the wire structures is broadened when development time is increased. Resist swelling might occur for long development since it can induce physical deformation and additional stress. It should be noted that exposure dose and development time are interrelated to each other as short exposure and long development can be equal to heavier development and short development.

Development type is also a critical effect on maintainability, robustness, and reproducibility. When development process is performed with type of MIBK: IPA (1:3), it is seen that the amount of gap in the interwire region is likely to be obtained to large extent due to having the feature of high resolution for MIBK: IPA (1:3), but not very well sensitivity. However, when the developer process is occurred on MIBK: IPA (1:1) along with MIBK: IPA (1:3), the possibility of opening all gap structures between the electrode is being decreased. The reason is that the condition in which the dilution rate is selected as MIBK: IPA (1:1) and proceeded with MIBK: IPA (1:3), creates a fast development process, resulting in overdeveloped for resolution of nanostructures although patterns are cleaned sufficiently in terms of sensitivity. In case of incorporating higher concentration along with lower concentration developer types, only highly exposed areas can remain on the substrate.

Bake temperature is a decisive influence on the fabrication process because of removing the amount of solvent and strengthening the adhesion of the resist to substrate. The length of the gap region is increased as the baked temperature is increased due to the low linking of the polymer chain.

Another parameter, the substrate effect, directs the fabrication process based on what kind of substrate is preferred to see their influence in the process. In our work, silicon, glass and  $Si_3N_4$  grown on bare silicon show different responses when related nanostructures are fabricated onto them. Because of having an insulator feature in the glass substrate, the number of scattering events occurs frequently. Additionally, heating is another problem, especially in higher exposure dose. Taking into these drawbacks for glass, it is seen that linewidth of nanostructures in which all structures are patterned on the glass substrate is

broader. Additionally, when the same structures are manufactured on the substrate of silicon and  $Si_3N_4$  grown on bare silicon, because the atomic number of  $Si_3N_4$  is less than Si, it leads to less scattering effect and so, line variations in patterns are observed very less.

The last parameter is related to the package of proximity effect correction (PEC) which is algorithm classifying dose range into related structures based on point spread function (PSF) used for PEC calculation is driven by Monte Carlo simulation. The main idea for PEC is to deliver lower doses in dense regions and higher doses in isolated regions to provide equalization through a nanostructure. If the sensitive pattern in terms of dimension includes PEC, acquiring the length of structures has less variation and the chance of getting strong patterns is getting increased physically.

## BIBLIOGRAPHY

- [1] R. K. Cavin, P. Lugli, and V. V Zhirnov, "Science and engineering beyond Moore's law," *Proc. IEEE*, vol. 100, no. Special Centennial Issue, pp. 1720–1749, 2012.
- [2] B. Bhushan, *Springer handbook of nanotechnology*. Springer, 2017.
- [3] S. E. Thompson and S. Parthasarathy, "Moore's law: the future of Si microelectronics," *Mater. today*, vol. 9, no. 6, pp. 20–25, 2006.
- [4] G. M. Whitesides, "Nanoscience, nanotechnology, and chemistry," *Small*, vol. 1, no. 2, pp. 172–179, 2005.
- [5] C. M. Niemeyer, "Nanoparticles, proteins, and nucleic acids: biotechnology meets materials science," *Angew. Chemie Int. Ed.*, vol. 40, no. 22, pp. 4128–4158, 2001.
- [6] G. Acar, O. Ozturk, A. J. Golparvar, T. A. Elboshra, K. Böhringer, and M. K. Yapici, "Wearable and flexible textile electrodes for biopotential signal monitoring: A review," *Electronics*, vol. 8, no. 5, p. 479, 2019.
- [7] L. Lombardo, "Nanowire biosensor as cost-effective testing platform for biomedical applications," Politecnico di Torino, 2018.
- [8] S. F. A. Ragman, N. A. Yusof, U. Hashim, and N. M. Nor, "Design and fabrication of silicon nanowire based sensor," *Int. J. Electrochem. Sci*, vol. 8, pp. 10946–10960, 2013.
- [9] A. E. Grigorescu and C. W. Hagen, "Resists for sub-20-nm electron beam lithography with a focus on HSQ: state of the art," *Nanotechnology*, vol. 20, no. 29, p. 292001, 2009.
- [10] M. A. Mohammad, M. Muhammad, S. K. Dew, and M. Stepanova, "Fundamentals of electron beam exposure and development," in

*Nanofabrication*, Springer, 2012, pp. 11–41.

- [11] C. S. Wu, Y. Makiuchi, and C. Chen, *High-energy electron beam lithography for nanoscale fabrication*. InTech Europe: Rijeka, Croatia, 2010.
- [12] A. A. Tseng, K. Chen, C. D. Chen, and K. J. Ma, “Electron beam lithography in nanoscale fabrication: recent development,” *IEEE Trans. Electron. Packag. Manuf.*, vol. 26, no. 2, pp. 141–149, 2003.
- [13] T. Newman, “Tiny tale gets grand, California Institute Technol.,” *J. Eng. Sci.*, vol. 49, p. 24, 1986.
- [14] J. R. Arthur Jr, “Interaction of Ga and As<sub>2</sub> molecular beams with GaAs surfaces,” *J. Appl. Phys.*, vol. 39, no. 8, pp. 4032–4034, 1968.
- [15] D. M. Eigler and E. K. Schweizer, “Positioning single atoms with a scanning tunnelling microscope,” *Nature*, vol. 344, no. 6266, p. 524, 1990.
- [16] MicroChem, “No Title,” *MicroChem*, p. 4.
- [17] N. Pidgeon *et al.*, “Nanoscience and nanotechnologies: opportunities and uncertainties,” *R. Soc. R. Acad. Eng.*, vol. 29, no. 07, p. 2004, 2004.
- [18] L. Filipponi and D. Sutherland, “Nanotechnologies: principles, applications, implications and hands-on activities,” *Publ. Off. Eur. Union, Luxemb.*, 2013.
- [19] J. Kim, S. Qin, W. Yao, Q. Niu, M. Y. Chou, and C.-K. Shih, “Quantum size effects on the work function of metallic thin film nanostructures,” *Proc. Natl. Acad. Sci.*, vol. 107, no. 29, pp. 12761–12765, 2010.
- [20] G. Rius Suñé, *Electron beam lithography for nanofabrication*. Universitat Autònoma de Barcelona, 2008.
- [21] R. J. Behm, N. García, and H. Rohrer, *Scanning tunneling microscopy and related methods*, vol. 184. Springer Science & Business Media, 2013.
- [22] Z. Cui, *Micro-nanofabrication: technologies and applications*. Springer, 2006.
- [23] D. L. Tolliver, *Handbook of contamination control in microelectronics*:

*principles, applications, and technology*. William Andrew Publishing, 1988.

- [24] J. Kim, “A Study of Fabrication of Ultra-high Resolution Nano Devices through Electron Beam Lithography Process and Its Application to Electron–Optical Systems,” 2007.
- [25] A. Pimpin and W. Srituravanich, “Review on micro-and nanolithography techniques and their applications,” *Eng. J.*, vol. 16, no. 1, pp. 37–56, 2012.
- [26] B. Cui, *Recent advances in nanofabrication techniques and applications*. BoD–Books on Demand, 2011.
- [27] K. I. Nura Liman Chiromawa, “Applications of Electron Beam Lithography (EBL) in Optoelectronics Device Fabrication.,” *AASCIT J. Phys.*, vol. 4, no. 2, p. 5, 2018.
- [28] Y. Chen and A. Pepin, “Nanofabrication: Conventional and nonconventional methods,” *Electrophoresis*, vol. 22, no. 2, pp. 187–207, 2001.
- [29] R. C. Jaeger, *Introduction to microelectronic fabrication*, vol. 2. Prentice Hall Upper Saddle River, NJ, 2002.
- [30] J. Chopra, “Analysis of lithography based approaches in development of semi conductors,” *arXiv Prepr. arXiv1502.05887*, 2015.
- [31] J. R. Maldonado and M. Peckerar, “X-ray lithography: Some history, current status and future prospects,” *Microelectron. Eng.*, vol. 161, pp. 87–93, 2016.
- [32] P. Rai-Choudhury, *Handbook of microlithography, micromachining, and microfabrication: microlithography*, vol. 1. Iet, 1997.
- [33] A. A. Tseng, “Recent developments in micromilling using focused ion beam technology,” *J. micromechanics microengineering*, vol. 14, no. 4, p. R15, 2004.
- [34] J. Melngailis, A. A. Mondelli, I. L. Berry III, and R. Mohondro, “A review of ion projection lithography,” *J. Vac. Sci. Technol. B Microelectron. Nanom. Struct. Process. Meas. Phenom.*, vol. 16, no. 3, pp. 927–957, 1998.
- [35] S. Barcelo and Z. Li, “Nanoimprint lithography for nanodevice fabrication,”

*Nano Converg.*, vol. 3, no. 1, p. 21, 2016.

- [36] A. Abbas, “Nanofabrication Using Electron Beam Lithography: Novel Resist and Applications,” University of Waterloo, 2013.
- [37] J. Zhou and X. Yang, “Monte Carlo simulation of process parameters in electron beam lithography for thick resist patterning,” *J. Vac. Sci. Technol. B Microelectron. Nanom. Struct. Process. Meas. Phenom.*, vol. 24, no. 3, pp. 1202–1209, 2006.
- [38] D. C. Leitao *et al.*, “Optimization of exposure parameters for lift-off process of sub-100 features using a negative tone electron beam resist,” in *2012 12th IEEE International Conference on Nanotechnology (IEEE-NANO)*, 2012, pp. 1–6.
- [39] A. van de Kraats and R. Murali, “Proximity effect in e-beam lithography,” *Atlanta, Georg. Nanotechnology Res. Center, Georg. Inst. Technoogy*, 2005.
- [40] N. Yao and Z. L. Wang, *Handbook of microscopy for nanotechnology*. Springer, 2005.
- [41] MicroChem, “No Title.”
- [42] Y. Chen, “Nanofabrication by electron beam lithography and its applications: A review,” *Microelectron. Eng.*, vol. 135, pp. 57–72, 2015.
- [43] M. Altissimo, “E-beam lithography for micro-/nanofabrication,” *Biomicrofluidics*, vol. 4, no. 2, p. 26503, 2010.
- [44] A. N. Broers, “Resolution limits for electron-beam lithography,” *IBM J. Res. Dev.*, vol. 32, no. 4, pp. 502–513, 1988.
- [45] J. Bolten *et al.*, “Improved CD control and line edge roughness in E-beam lithography through combining proximity effect correction with gray scale techniques,” *Microelectron. Eng.*, vol. 87, no. 5–8, pp. 1041–1043, 2010.
- [46] K. Liu, P. Avouris, J. Bucchignano, R. Martel, S. Sun, and J. Michl, “Simple fabrication scheme for sub-10 nm electrode gaps using electron-beam lithography,” *Appl. Phys. Lett.*, vol. 80, no. 5, pp. 865–867, 2002.

- [47] A.-P. Blanchard-Dionne and M. Meunier, "Electron beam lithography using a PMMA/P (MMA 8.5 MAA) bilayer for negative tone lift-off process," *J. Vac. Sci. Technol. B, Nanotechnol. Microelectron. Mater. Process. Meas. Phenom.*, vol. 33, no. 6, p. 61602, 2015.
- [48] M. Nuzaihan *et al.*, "Top-down nanofabrication and characterization of 20 nm silicon nanowires for biosensing applications," *PLoS One*, vol. 11, no. 3, p. e0152318, 2016.
- [49] S. H. Oh, J. G. Kim, C. S. Kim, D. S. Choi, S. Chang, and M. Y. Jeong, "The fabrication of 3-D nanostructures by a low-voltage EBL," *Appl. Surf. Sci.*, vol. 257, no. 9, pp. 3817–3823, 2011.
- [50] M. S. N. Humaira, U. Hashim, T. Nazwa, S. T. Ten, S. Ahmad, and N. A. Yusof, "Process development of 40 nm silicon nanogap for sensor application," in *2014 IEEE International Conference on Semiconductor Electronics (ICSE2014)*, 2014, pp. 96–99.
- [51] C. Vieu *et al.*, "Electron beam lithography: resolution limits and applications," *Appl. Surf. Sci.*, vol. 164, no. 1–4, pp. 111–117, 2000.
- [52] H. Elsner and H.-G. Meyer, "Nanometer and high aspect ratio patterning by electron beam lithography using a simple DUV negative tone resist," *Microelectron. Eng.*, vol. 57, pp. 291–296, 2001.
- [53] D. R. S. Cumming, S. Thoms, J. M. R. Weaver, and S. P. Beaumont, "3 nm NiCr wires made using electron beam lithography and PMMA resist," *Microelectron. Eng.*, vol. 30, no. 1–4, pp. 423–425, 1996.
- [54] S. Yasin, D. G. Hasko, and H. Ahmed, "Fabrication of < 5 nm width lines in poly (methylmethacrylate) resist using a water: isopropyl alcohol developer and ultrasonically-assisted development," *Appl. Phys. Lett.*, vol. 78, no. 18, pp. 2760–2762, 2001.
- [55] C. Yanik, "Fabrication and charge transport measurements on graphene-based nanostructures in the quantum hall regime," 2016.

- [56] G. Owen, "Electron lithography for the fabrication of microelectronic devices," *Reports Prog. Phys.*, vol. 48, no. 6, p. 795, 1985.
- [57] K. Indykiewicz, B. Paszkiewicz, and R. Paszkiewicz, "Substrate Effect in Electron Beam Lithography," *Adv. Electr. Electron. Eng.*, vol. 16, no. 2, pp. 246–252, 2018.
- [58] C.-H. Seo and K.-Y. Suh, "Reduction of proximity effect in electron beam lithography by deposition of a thin film of silicon dioxide," *Korean J. Chem. Eng.*, vol. 25, no. 2, pp. 373–376, 2008.
- [59] T. Yamaguchi, H. Namatsu, M. Nagase, K. Yamazaki, and K. Kurihara, "A new approach to reducing line-edge roughness by using a cross-linked positive-tone resist," *Jpn. J. Appl. Phys.*, vol. 38, no. 12S, p. 7114, 1999.

## APPENDIX A

### OPERATING PROCEDURE FOR VISTEC EBP5000+ES



Figure A.1 Vistec EBP5000+ES 100 kV Electron Beam Lithography System at Sabancı University Nanotechnology Research and Application Center's (SUNUM) clean-room [55]

- Monitor the system conditions by checking the “CSYS”.
- Vent the airlock by pushing the “set lock vent” button in “CSYS”. After between 2-3 min., airlock reaches the atmospheric pressure as seen in Fig.A.2a.
- Remove the cassette holder as illustrated in Fig.A.2b.
- In the cassette, there are 2 types of “cassette holder”. Cassette 1 placed in the upper side is related to mask holder and Cassette 2, in the downside, is corresponds to fabricate samples
- You should put the cassette into EBL machine and press set lock vacuum in the CSYS. Check the O-ring
- While you are carrying holder, do not touch the calibration marker and faraday marker as shown in Fig.A.2c.

- Fig.A.2c demonstrates two parts in the cassette 2, low-x and high-y. You can put your sample in one of the parts via clipping with sample clips.
- Adjust the sample orientation carefully. After making sure that replace your sample carefully, put the holder to the microscope stage
- Holder is clamped in the tray by turning the screws in the counterclockwise direction as illustrated in Fig.A.2e.
- Microscope and laser meter are opened. Going to the faraday cup, the center of the faraday cup has put the cross as demonstrated in Fig.A.2e.
- Position meter, Fig.A.2d, of X and Y is made as Zero. After initializing, all movements will be made relative to the faraday cup.
- Adjust the height with the three leveling set screws. By turning the clockwise direction fully, the stage will go down approximately 200  $\mu\text{m}$ . Height should be between -50  $\mu\text{m}$  to 50  $\mu\text{m}$  range. It depends on the dimension of the sample. If you have a sample that is 1 cm  $\times$  1 cm, the height difference should not be bigger than 10  $\mu\text{m}$ .
- After making height adjustment, both coordinates from the edge of the samples as X1; X2 and Y1; Y2 are taken and added them up and dividing by 2. The center of your substrate as (X0; Y0) is calculated. Remove the holder. Do not forget to release the "release lever"
- The vacuum of the system is broken by pressing the vent the lock button again. Place holder the holder to the cassette as seen in Fig.A.2g.
- Cassette is placed to the airlock and then you will hear a "click" voice when it is plugged properly.
- We must wait until vacuum reaches the minimum required value of  $5 \times 10^{-5}$  TORR.
- When it reached to required vacuum level, part of the airlock region in CSYS is turned into green and CEBPG will be highlighted as demonstrated in Fig.A.2h.
- The holder type which is Lowy (3) or Highly (2) can be selected and the process is started to load the holder by pressing arrow icon under the cassette in "Cebpg"
- GPF file is copied from the LayoutBeamer-Machine folder on the desktop and pasted it to the pattern file of your account
- To change the environment, open the new terminal and enter the "ce username" command

- Command of “Set”, “Measure” or “Adjust” is never given if there is no holder inside the system.
- Enter the command of “cjob” after changing the environment, then create my job file.
- To reach achieved current in the system, enter the command of “iarc beam”. To load the desired current, you can double click for that current.
- To find the marker on the holder, “mvm” should be entered
- After finding the marker, the command of “atc” should be entered.
- “mcur” as short command should be entered to measure the amount of loading current
- Since we are in the faraday cup as 0,0 position, we can enter the coordinates of  $X_0, Y_0$  relative from the faraday cup by giving command of mpos /r  $X_0, Y_0$ .
- To check whether you are on the substrate or not, just enter the “mpgm height”. If the result is in the micron range, you are on the substrate.
- By entering the command of “mpg tab”, the coordinate of this point can be taken relative to the reference point.
- Coordinate of this point is copied and pasted to parameters part in "Cebpg", and choose your file, submit it then drag the panel bar down to start the exposure.
- When you finish all processes, leave the system at the low current such as 0.5 nA, 1 nA, etc to avoid damage for beam-blanker.

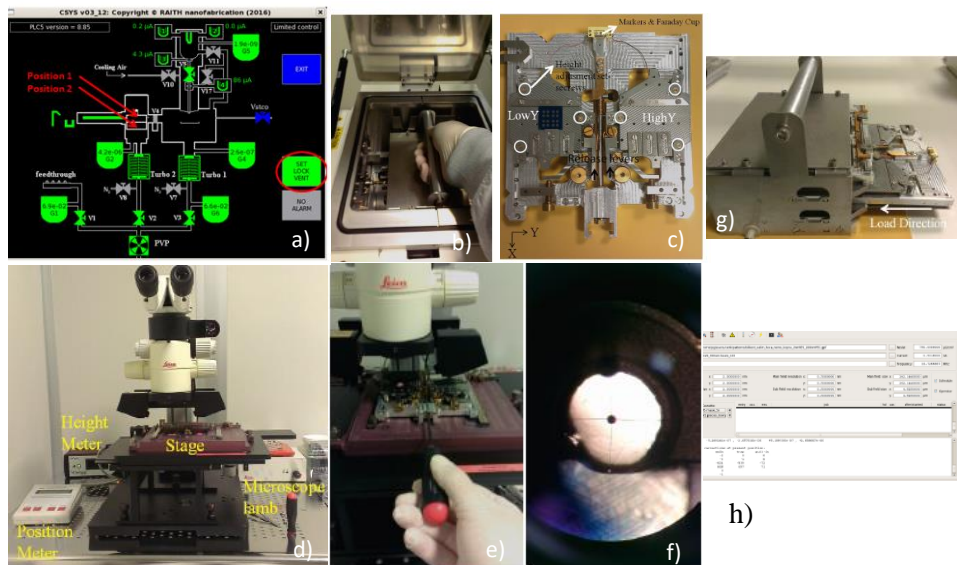


Figure A.2 Pieces of Electron Beam Lithography (EBL) and Operating Flow [55]